國立交通大學

資訊科學與工程研究所

碩 士 論 文

探討環境參照系與自我參照系於空間巡航中腦波反應之差異

Differences in EEG Dynamics between the use of Allocentric and Egocentric reference frames during VR based Spatial Navigation

研 究 生：邱德正

指導教授：林進燈 教授

中 華 民 國 九 十 七 年 七 月

探討環境參照與自我參照系

於空間巡航中腦波反應之差異

Differences in EEG Dynamics between the use of Allocentric and Egocentric reference frames during VR based Spatial Navigation

研 究 生：邱德正　　Student: Te-Cheng Chiu

指導教授：林進燈 教授　　Advisor: Prof. Chin-Teng Lin

國 立 交 通 大 學

資 訊 科 學 與 工 程 研 究 所

碩 士 論 文

A Thesis
Submitted to Institute of Computer Science and Engineering
College of Computer Science
National Chiao Tung University
in partial Fulfillment of the Requirements
for the Degree of
Master
in
Computer Science
July 2008
Hsinchu, Taiwan, Republic of China

中華民國九十七年七月

探討環境參照系與自我參照系
於空間巡航中腦波反應之差異

學生：邱德正　　指導教授：林進燈 博士

國立交通大學資訊科學與工程研究所

中文摘要

空間巡行(spatial navigation)的策略，可依照參照系(reference frame)的不同，分成自我(egocentric)和環境(allocentric)兩種空間表示方式。本研究以腦電波(EEG)探討汽車駕駛中，此兩種參照系於空間巡航中腦波反應之差異。本實驗利用虛擬實境(Virtual Reality)技術，建構3D虛擬場景，模擬真實的駕車環境。在實驗中以隧道為場景，以減少不必要的視覺刺激，探討此兩種參照系對空間描述的差異，藉此有效區分使用不同思考策略的受測者並進一步找出其腦波反映上的差異。在資料分析上，我們利用獨立成分分析(ICA)，將測量到的腦電波，分離成互相獨立的大腦訊號源，並以事件相關頻譜擾動(ERSP)之分析法，觀察自我參照系與環境參照系之間腦波頻率在時間上變化的差異。實驗結果發現，在自我參照系和環境參照系受測者之腦電波有顯著的差異。自我參照系的受測者，其大腦頂葉區(Parietal)在，在空間巡航時，有較強烈的反應。而環境參照系的受測者則是在枕葉區(Occipital)，在腦部重組巡行空間時，有較強烈的反應。除此之外，自我參照系的受測者，其大腦頂葉區(Parietal)在，在空間巡航時，其alpha波的能量強弱與其衡量空間巡行角度的正確性有高度的相關。此實驗結果幫助我們了解與空間巡行感知相關的腦神經網路，此一結果將有助於進一步探討不同策略受試者其空間迷向時的腦波變化，並能藉此發展出一套輔助裝置，協助受試者增進空間巡行時的能力，減少其發生空間迷向的機會。

關鍵詞: 空間巡行、自我參照系、環境參照系、腦電波、事件相關頻譜擾動、獨立成份分析

Differences in EEG Dynamics between the use of Allocentric and Egocentric reference frames during VR based Spatial Navigation

Student: Te-Cheng Chiu Advisor: Prof. Chin-Teng Lin

College of Computer Science
National Chiao Tung University

Abstract

The aim of this study was to investigate the differences of brain dynamics between the use of allocentric reference frames and egocentric reference frames during spatial navigation. A tunnel task was designed to classify subjects into allocentric or egocentric spatial representation users. Despite of the differences of mental spatial representation, behavioral performance in general were compatible between the two strategies subjects in the tunnel task. Task-related EEG dynamics in both tonic and phasic power changes were analyzed using independent component analysis (ICA), time-frequency and non-parametric static test. Results supported the dissociation brain activities between the uses of allocentric and egocentric reference frames. Both tonic and phasic power changes were significantly different between the navigation strategy groups. Subjects who preferred to use the allocentric spatial representation showed stronger activation in occipital area during path integration whereas subjects using the egocentric reference frames showed stronger activation in parietal area during path integration. The distinct brain regions involved in the navigation process suggested that encodings of allocentric and egocentric reference frames were via the ventral and dorsal neural network respectively.

Keyword: spatial navigation, allocentric, egocentric, reference frame, electroencephalograph (EEG), independent component analysis (ICA)

誌　　謝

本論文的完成，首先要感謝指導教授林進燈博士這兩年來的悉心指導，讓我學習到許多寶貴的知識，在學業及研究方法上也受益良多。另外也要感謝口試委員們的建議與指教，使得本論文更為完整。

特別感謝美國加州聖地牙哥大學的鐘子平教授、段正仁教授給予我研究上最大的協助，從實驗設計、實驗分析、實驗結果討論到論文撰寫，給我最專業的意見跟看法。

另外，我要感謝腦科學研究實驗室的全體成員，沒有他們也就沒有我個人的成就。特別感謝曲在雯博士給予我在各方面的指導，無論是研究上疑難的解答、研究方法、寫作方式、經驗分享等惠我良多。另外要感謝尚文、柏銓、玠瑤、青甫同學，在過去兩年研究生活中同甘共苦，相互扶持。此外，我也要感謝黃冠智學長、柯立偉學長、趙志峰學長、陳玉潔學姐、林君玲學姐、陳世安學長與黃騰毅學長在研究上的幫助，還有感謝 Frank、馥戍、建安、昂穎、睿昕、華山，在過去這一年中的相伴。同樣地也感謝實驗室助理在許多事務上的幫忙。

謹以本文獻給我親愛的家人與親友們，以及關心我的師長，願你們共享這份榮耀與喜悅。

Content

List of Figures

List of Tables

Chapter 1 Introduction

1.1 Background

Spatial navigation is a crucial ability for living, since way-finding and environment exploration always happens in our daily life. Moreover, we need traveling around places to access all kinds of resources, and it made the ability to navigate in the environment essential and became a part of living (Darken and Sibert, 1996). Spatial navigation is a complex task which requires to integrate information from different sensory inputs and to construct the spatial representation of the environment. Different ways of interaction of reference frames can be used to maintain the orientation and position during navigation, such as path integration and piloting (Dourish and Chalmers, 1994; Darken and Sibert, 1996; Darken and Peterson, 2001). According to the computation of reference of frames, there are two classes of internal spatial representation systems: the allocentric representation system and the egocentric representation system (Panti and Dupree, 1994; Howard and Templeton, 1966; Lacquaniti, 1997). In the egocentric reference system, the spatial location of an object is specified with respect to the navigator or observer. The spatial representation of an object depends on the position or orientation of the observer and the representation changes along with the observer's position or orientation. On the other hand, the spatial location of an object is referred by the relationship between object to each other in the allocentric reference system. People who prefer to use an allocentric reference frame describe the spatial location of an object with respect to features or landmarks of the environment (Darken and Peterson, 1996; Klatzky, 1998). In contrast to egocentric system, the spatial location of an object represented by allocentric reference frame is independent on the location and orientation of observer.

In summary, the spatial representation of an object is body-based in egocentric reference system but it is object-based in allocentric reference system (Darken and Peterson, 1996; Klatzky, 1998).

Visuospatial navigation is a task that involves complex cognitive functions which employ multiple brain regions. Brain activations in bilateral hemisphere including frontal, parietal, pre-motor, occipital, and temporal areas revealed an association with spatial navigation (Maguire et al., 1998; Grön et al., 2000; Shelton and Gabrieli, 2002; Ekstrom et al., 2003). For example, some studies demonstrated the importance of the parietal region in maintaining the performance of the spatial navigated in the environment. The place cells, exhibited in the hippocampus of the animals and human, have also known to play an important role to maintain cognitive map of spatial environment (Maguire et al., 1998). Moreover, patients with brain damage covered the parietal and hipoocampus regions were impaired the ability of spatial navigation in the environment (Gilbert et al., 1998; Rosenbaum et al., 2000; Moscovitch et al., 2005, 2006; Maguire et al., 2006).

EEG studies showed that neural rhythms in alpha band and theta band were particularly associated with visuospatial task (Kahana et al., 1999; Raghavachari et al., 2001; Caplan et al., 2003; Buzsáki, 2005). For example, the alpha band power was stronger during navigation in complex mazes than that during navigated in simple mazes. Klaus also reported that the alpha power attenuated during path integration. The change of alpha rhythm was suggested to be an index of navigation related cortical activation. Some studies, especially the ECoG signals, found that theta rhythm might encode the spatial representation and the increased theta oscillation was observed at cortical areas including temporal, frontal, and parietal regions during spatial navigation. The neuropsychological studies suggested the functional

dissociation between the use of allocentric and egocentric reference frames (Vallar et al., 1999; Ota et al., 2001; Fink et al., 2003; Gramann et al., 2006). Specifically, neural image studies showed that the use of egocentric reference frame exhibits stronger activation in frontal, parietal and premotor cortex. A fronto-parietal network or parietal-premotor network also suggested to be involved in processing the egocentric information (Mellet et al., 2000; Galati et al., 2000; Committeri et al., 2004; Gramann et al., 2006; Zaehle et al., 2007). However,, the activation of a network comprised the parietal area, occipito-temporal area (Gröne et al., 2000; Shelton and Gabrieli, 2002; Jordan et al., 2004; Gramann et al., 2006; Zaehle et al., 2007) including parahippocampal region, hippocampus, and thalamus (Jordan et al., 2004) were found to encoded the allocentric based space representation.

Computer-simulated virtual world provides an effective and flexible way to investigate the human behavioral and brain activities during navigation in different space scale and complexity of environments including city, town, room and maze (Grön et al., 2000; Janzen and van Turennout, 2004; Jordan et al., 2004). For example, research on exploring the substrate of neural network which associated with navigation in a virtual maze found theta activity among frontal, parietal and temporal cortex. Some studies used the virtual city to investigate the brain activity correlates to spatial learning and different spatial navigation strategies (Maguire et al., 1998; Ekstrom et al., 2003; Maguire et al., 2006). However, during navigated through the environment, we often rely on a plenty of cues for planning large-scale movements (such as walking through the environment), for combining trajectories of previously traveled paths into a mental representation of the environment, and for determining heading. Previous studies also showed that subjects' navigation strategies were easily biased by the environmental cues when navigated in a complex virtual environment

(Darken and Sibert, 1996). Therefore, it is hard to clearly relate the brain activations between the use of allocentric and egocentric reference frames in a complex virtual world. The line bisection task (Vallar et al., 1999; Fink et al., 2003; Committeri et al., 2004; Gramann et al., 2006; Zaehle et al., 2007) which use the static stimuli, was designed for investigating the distinct brain activations that specifically involved in allocentric and egocentric reference frame system. However, this static task may still insufficient to investigate dynamic brain activity associated with navigation.

.1.2 Aim of this thesis

The aim of this study is to characterize the detailed differences in EEG dynamics between subjects who use an egocentric and allocentric reference frames. We designed a tunnel task (Gramann et al., 2006) to distinguish subjects using the egocentric reference frames from subjects using the allocentric reference system during spatial navigation. The tunnel task was built in a 3D virtual reality based driving-simulation environment. Since there was no extra landmarks in the tunnel, subjects' navigation strategies were not biased by the environment and therefore we could classify subjects into two different navigation strategy groups according to their use of cognitive reference frames while passing through the tunnel. The 32-channel EEG activities were recorded during subjects navigated in the tunnel and responded to the homing direction selections and homing angular estimation. EEG signals were processed and revealed in the spectro-temporal domain. Effects of the navigation strategy and turning degree on neural rhythms in different brain regions were compared and assessed in details.

Chapter 2 Experimental Apparatus

2.1 Experimental Setup

The experiment was performed in an interactive virtual reality (VR) driving environment (Fig. 2-1A). Subjects sat comfortably in a car (without the unnecessary weight of the engine and other components), which was mounted in the center of a dimmed quiet room. The VR based driving environment was constructed by five projection screens circularly surround the car with a distance of 100 cm and provided 206° frontal field of view (FOV), and 40° back FOV to construct. The realistic scenery and physic simulation were constructed with the World Tool Kit (WKT) library which is a well-known tool to build a virtual world. Two buttons were placed on the steering wheel (Fig. 2-1C), and subjects could interact with the environment by pressing the buttons. The button pressed signals were wirelessly transmitted to a computer which was used to collect the environment events synchronized EEG signals. The experimental processes were recorded by the video camera for monitoring and evaluating the subject's conditions.

Figure 2-1: The dynamic VR driving environment. (A): the photograph shows the 3D surrounded VR scene. (B): the photograph shows the Stewart platform. (C): the photograph shows locations of the buttons for subjects to select the homing direction and angle.

2.2 Subjects and EEG Recording

A total of 20 right-handed subjects were paid to participate in this study (age: 20-28 years, mean: 25 years). None of subjects had a history of neurological or psychiatric diseases and they were free from drug or alcohol abuse. No subjects reported with sleep deprivation at least at one day before the experiment. All participants were with normal or corrected to normal vision. All the setup and the

experimental protocols were approved by the Institutional Review Broad of Taipei Veterans General Hospital. Each subject was well instructed the procedures of experiment and none of them were aware of the experiment hypotheses. Subjects were sign the informed consent to before the experimental onset.

Subjects were with a movement-proof electrode cap sintered with 36 Ag/AgCl electrodes (Fig. 2-2B) for measuring the electrical activates of the brain and that is the electroencephalogram (EEG).

Figure 2-2: Photographs show the EEG amplifier (the NuAmps express system) and the displacement of the EEG cap.

All electrodes were placed in an elastic cap according to the international 10-20 system which was proposed by Jasper in 1958 (Fig. 2-3). The contact impedance between EEG electrodes and scalp was calibrated to be less than 5kΩ with conductive gel made by Compumedics. EEG data were recorded and amplified with the Scan NuAmps Express system (Compumedics Ltd., VIC, Australia) and sampled at 1000 Hz and 16-bit quantization level.

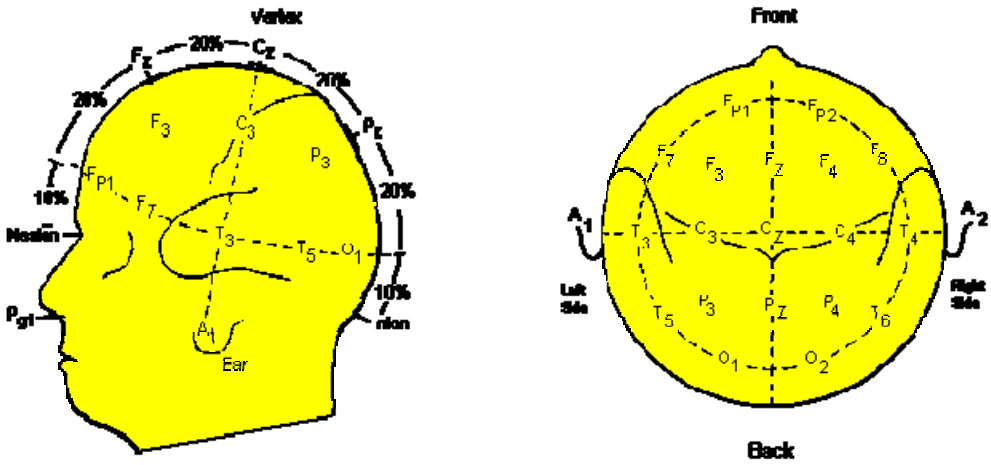

Figure 2-3: Pictures show the International 10-20 system of the electrode placement. (A): lateral view. (B): top view. (http://faculty.washington.edu/chudler/1020.html) .

At the end of the experiment, locations of electrodes were digitized with the 3D digitizer (POLHEMUS 3 space Fastrak). Fig. 2-4 shows the 3D digitizer system.

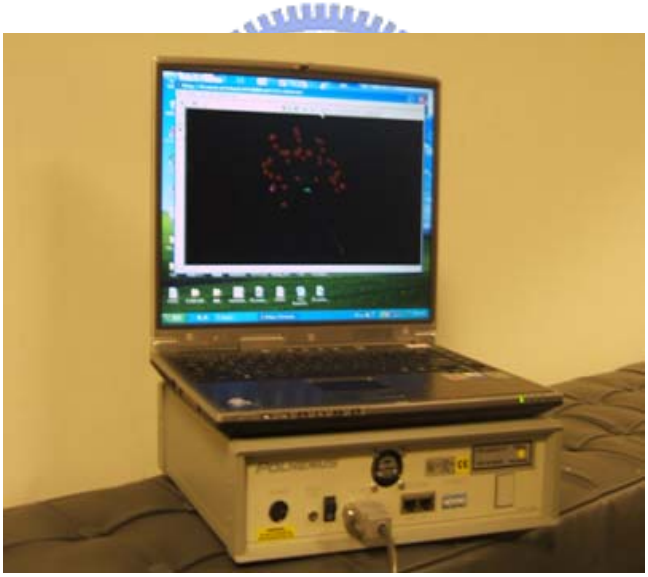

Figure 2-4: The picture shows the 3D Digitizer system which is for digitizing the positions of electrodes. The positions of each electrode are shown as red points on the screen.

2.3 Experimental Paradigm

The VR based tunnel-driving environment was used to investigate the EEG dynamics in spatial navigation. Animations of passages through a 3D virtual tunnel

consisting of a curve segment, which is between the two straight segments. were presented on the screen to simulate automatic car driving with a constant velocity. The VR scene only provided subjects with visual flows of spatial translation and rotation. No other landmarks or references existed in the tunnel scenery to bias subject's navigation strategy. The curve segment of the tunnel scene was randomly turned left or right in the degree of 30, 60, and 90. Subjects were required to keep the track of their implied virtual 3-D position with respect to their starting position during passage. At the end of each passage, a three dimensional homing arrow was appeared in the empty space in front of subject and subjects were required to indicate the homing direction by pressing the left or right buttons and the arrowhead was pointed roughly in the direction of the tunnel origin. The selection of the homing direction was associated with the subject's navigation strategy, the use of the reference frame. For example, for a right turn task, subjects with allocentric reference fame would indicate that the original entrance was in his left hand-side. Once the subject pressed the button to point the homing direction, the arrow started to rotate from 0 degree until subjects pressed the button again and the arrow was stopped and pointed to the estimating homing angle. Subjects were asked to practice the task at least for 5 min until familiar with the task. Each subject was required to complete four 20-minute sessions in the experiment and each session contained about 45 trails. Between two sessions, subjects could take rest for about 5-10 minutes.

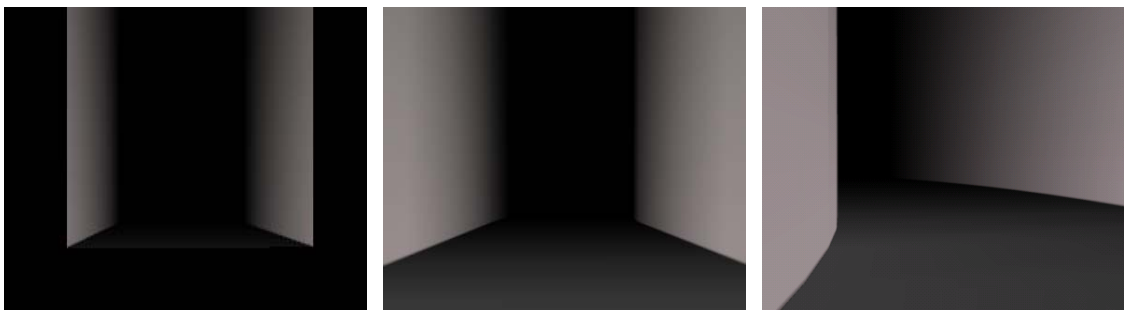

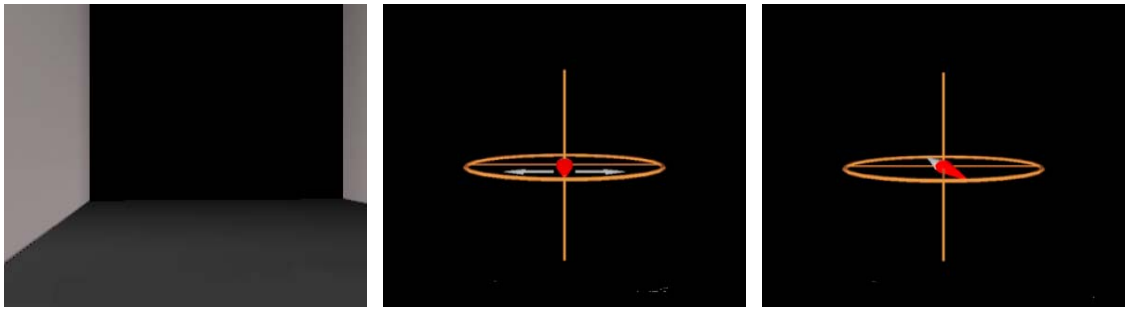

Figure 2-5: The episodes of virtual tunnel environment. (A): the entrance; (B): the forthright segment; (C): the meander segment; (D): the exit; (E): the cue for indicating homing direction and (F): the cue for indicating homing angle.

Fig. 2-6 shows the differences on the homing direction and angle between the egocentric and allocentric subjects. The homing direction is an index for differentiating the navigation strategies.

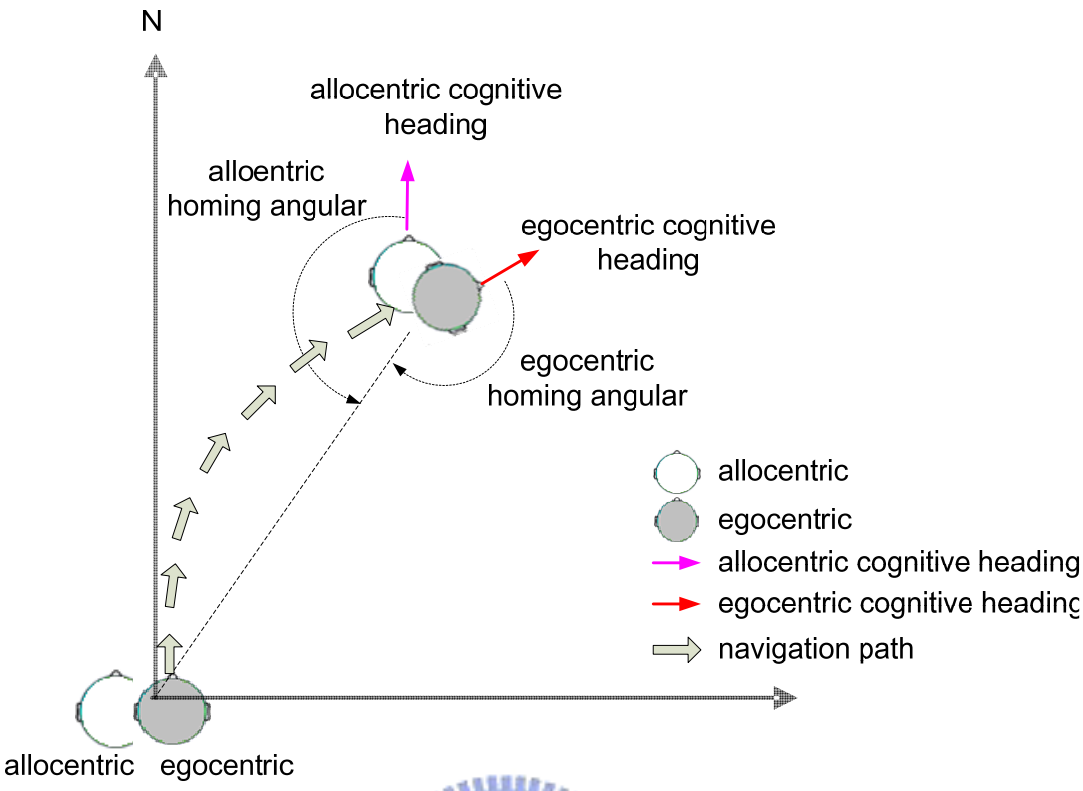

Figure 2-6: Picture shows the differences on the homing direction and angle between the egocentric and allocentric subjects. In the beginning, both allocentric and egocentric subjects are heading to north. At the end position, they have different cognitive heading directions. For allocentric subjects, the original place is located at the right-hand side of their cognitive heading, while the original place is located at the left-hand side of the egocentric subjects' cognitive heading.

Chapter 3 Data Analyses

All data was analysis by the tool of MATLAB and EEGLAB. MATLAB is a popular numerical analysis, statistic and scientific computing software and it is developed by MathWorks. The EEGLAB developed by Swartz Center for Computational Neuroscience (SCCN) of UCSD is a powerful MATALB toolbox for processing EEG data.

.3.1 Behavioral Data Analysis

Subjects who used the allocentric reference frame would point left for homing direction in a right turn, and point right in a left turn. On the other hand, subjects who used the egocentric reference frame would indicate the opposite homing directions. Subjects had to consistently (i.e., in > 70% of the trials across all sessions) select one or the other homing direction to be classified as an allocentric subject or an egocentric subject respectively. Otherwise, subjects were rejected to further analysis.

To assess the differences on the task performance between subjects who use an allocentric and an egocentric reference frame, the response time of selecting the homing direction, the mean pointing error and the absolute mean pointing error were further analyzed across subjects. Trials with left turn were first simply mirrored and merged, and then trials with pointing error point more than 1.5 interquartile ranges (IQRs) were removed as outliers. A 2 x 3 repeated-measures ANOVA [factors of strategy (allocentric vs. egocentric) and turning angle (30°, 60°, 90°)] were used to access the influences of factors on task performance including the response time, men pointing error, and absolute mean pointing error.

3.2 EEG Data Analyses

The flowchart of processing step was shown in Fig. 3-1. EEG signals were first

down sampled to 250Hz for data compression. Then, the EEG signals were filtered with a low-pass and high-pass filter with the cut-off frequencies at 50 and 0.5 Hz to remove the line noise (60 Hz and its harmonic) and the DC drifting.

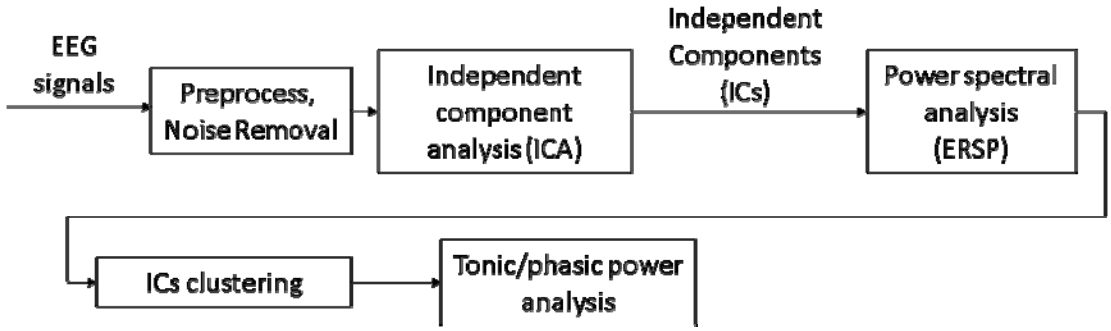

Figure 3-1: Picture shows the flowchart of EEG data analysis.

Artifacts contaminated in the EEG signals were first identified by visual inspection using the EEGLAB visualization tool and eliminated to enhance the signal to noise ratio. Those artifacts can be divided into physiologic and extra-physiologic activity (EEG Atlas: EEG Artifacts). The physiologic artifacts were generated from the subject, which rose from other sources instead of the brain (i.e., body movement, muscle activity). Extra-physiologic artifacts were contaminated from the equipment or the environment. Fig. 3-2 shows the examples of the some common artifacts contaminated in the EEG signals. Criteria used for artifacts rejection included extreme values, abnormal trends (linear drift) and abnormally distributed data.

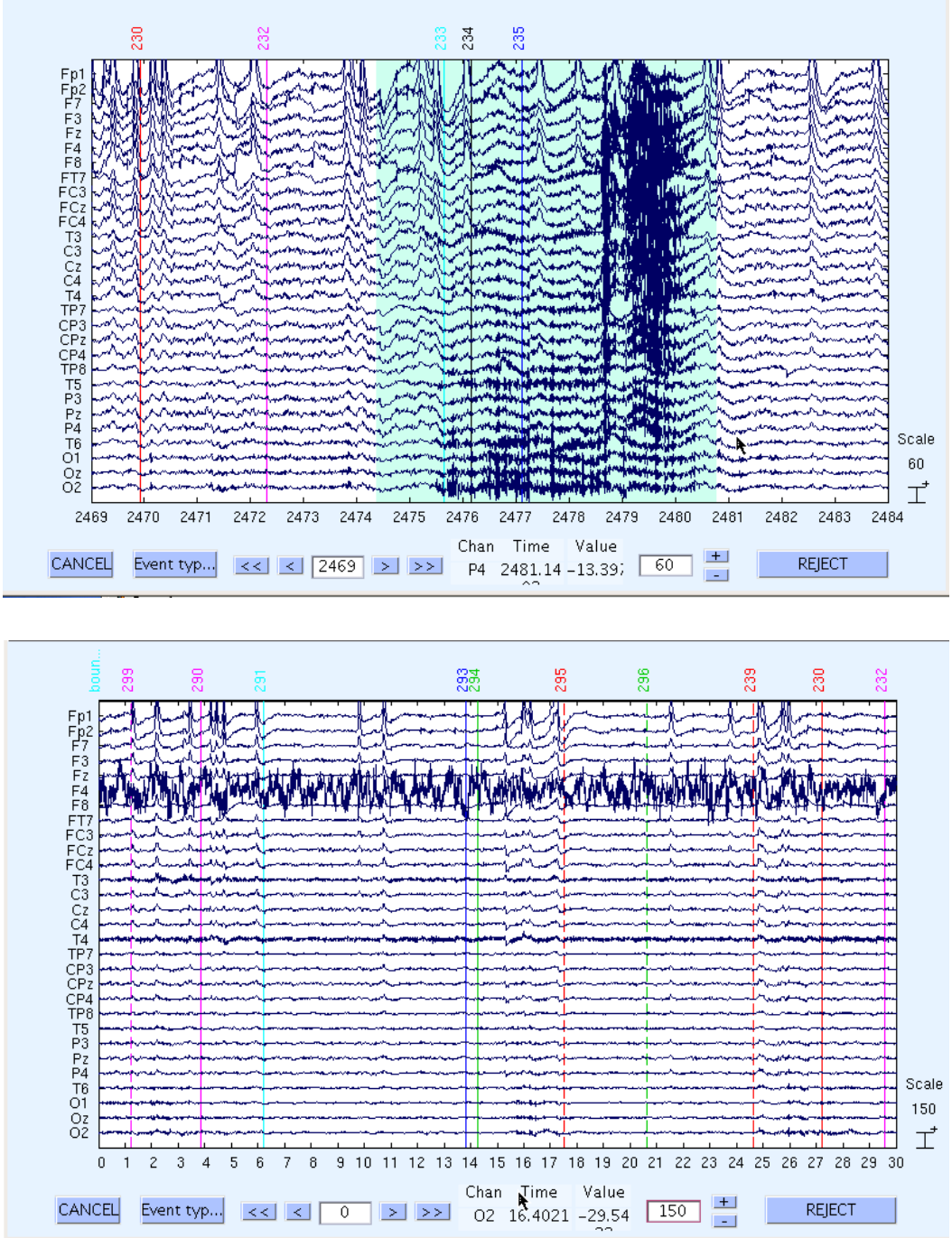

Figure 3-2: Pictures show the examples of common artifacts contaminated in the EEG signals. (A): artifacts from muscle activities. (B): artifacts from the bad channel F4.

The event-related potentials (ERPs) were then extracted from EEG data. Since turn segment of the tunnel scene contained with three different curve angles , the EEG responses related to different conditions (different navigation strategies and turn angles) were extracted and grouped separately. The extracted epochs were aligned to

the onset of turning of the tunnel scene for further analysis. The Fig. 3-3 shows methods for extracting and grouping epochs.

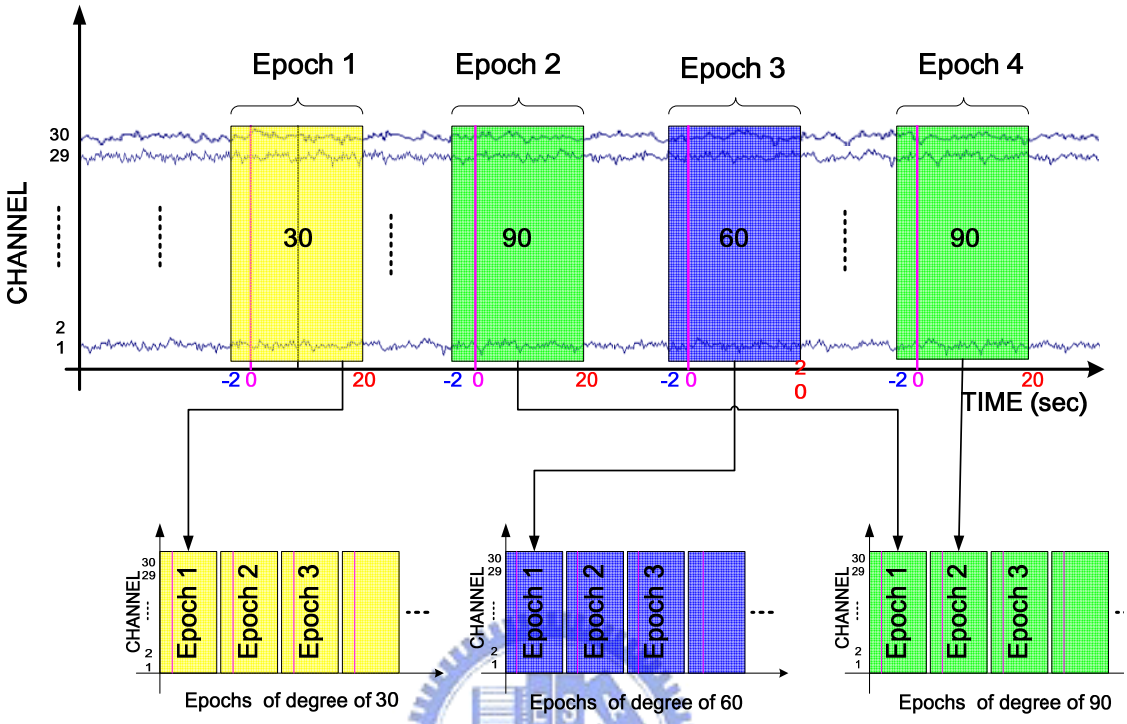

Figure 3-3: The picture shows the illustration of epoch extraction and grouping. The case-related ERPs are extracted from preprocessed EEG signals. The extracted epochs were polled and aligned by the onset of the turning segment.

The processed EEG signals were further separated into independent brain sources by independent component analysis (ICA) and the methods were briefly described in the following paragraph. ICA separated multichannel EEG data into statistically maximally independent components (ICs) arising from distinct brain area. The IC activities were used to assess the EEG dynamics in terms of spectro-temporal domain by using the event related spectral perturbation (ERSP) analysis.

3.3 Independent Component Analysis (ICA)

Each channel of EEG activities is a time course of mixed voltage activities which

collected from every point on scalp induces activity generated within a large brain area. Therefore, the EEG source segregation, identification, and localization were very difficult. Although brain tissue, cerebrospinal fluid, skull, and scalp lie between electrodes and cortex, the spatial smearing of EEG data by volume conduction did not cause significant time delay and it suggests that the ICA algorithm is suitable for performing blind source separation on EEG data. The ICA has extensively applied on blind source separation problem since 1990s (Rui et al.,2005; Jutten and Herault, 1991; Comon, 1994; Bell and Sejnowski, 1995) and the results (Makeig et al., 1996; Lee et al., 1999; Jung et al., 2000; Naganawa et al., 2005) demonstrated that ICA is a suitable solution to solve the problem of EEG source separation, identification, and localization. The ICA assumed that: (a) the conduction of the EEG sensors is instantaneously and linearly such that the measured mixing signals are linear and the propagation delays are negligible. (b) The signal source of muscle activity, eye movements, and, cardiac signals are not time locked to the sources of EEG activities which reflected the synaptic activities of cortical neurons.

$$\mathbf{x}(t) = \mathbf{A}\mathbf{s}(t) \tag{1}$$

$$\boldsymbol{u}(t) = \boldsymbol{W}\,\boldsymbol{x}(t) \tag{2}$$

ICA is a statistical and computational technique for revealing hidden factors that underlie sets of random variables, measurements, or signals and it describes the source separation problem as the form of equation (1). Where **x** is the signal recorded form scalp and ***A*** is a linear transform called a mixing matrix. Blind sources s_i are statistically mutually independent. The ICA model estimates a linear mapping ***W*** such that the unmixed signals ***u(t)*** are statically independent as in equation (2). In ideal case, ICA components ***u*** is equal or approximate to activity sources ***s***. Fig. 3-4 illustrates the concept of ICA application on EEG analysis.

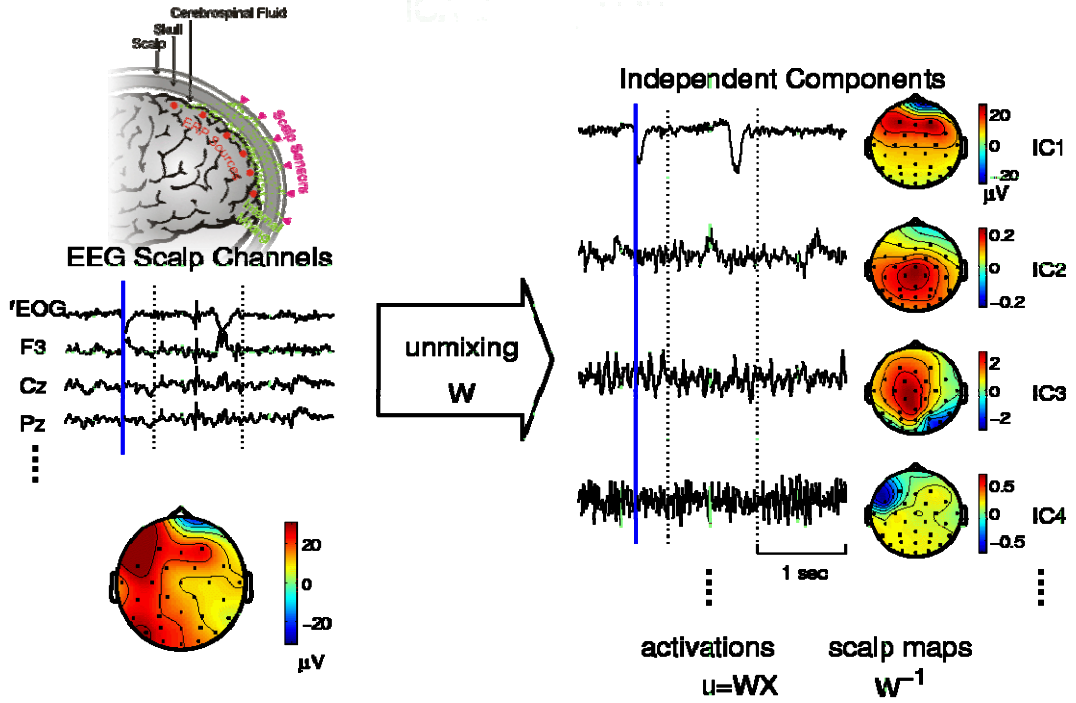

Figure 3-4: Picture shows the illustration of ICA decomposed concept. EEG signals recorded from the scalp are mixed with multiple sources by a mixing matrix. During the training phase, the ICA is to find a transformation to separate the mixed EEG signals into independent components which may have specific meanings. The transformation is specified by unmixing matrix $\boldsymbol{W}$ and scalp maps is able to plot according to the weight of $\boldsymbol{W}$.

In this study, we attempted to completely separate the twin problems of source identification and source localization by using a generally applicable ICA. Thus, the artifacts including the eye-movement (EOG), eye-blinking, heart-beating (EKG), muscle-movement (EMG), and line noises can be successfully separated from EEG activities. Fig. 3-5 shows the result of the scalp topographies of ICA weighting matrix $\boldsymbol{W}$ corresponding to each ICA component by projecting each component onto the surface of the scalp, which provided evidence for the components' physiological origins, e.g., eye activity was projected mainly to frontal sites, and the visual activity was on the occipital lobe, motor related potentials were located at the left and right

side of the parietal lobes, etc. The activities from different brain sources, eye movement artifacts, muscles and channel noises were effectively separated into independent components 1 and 30.

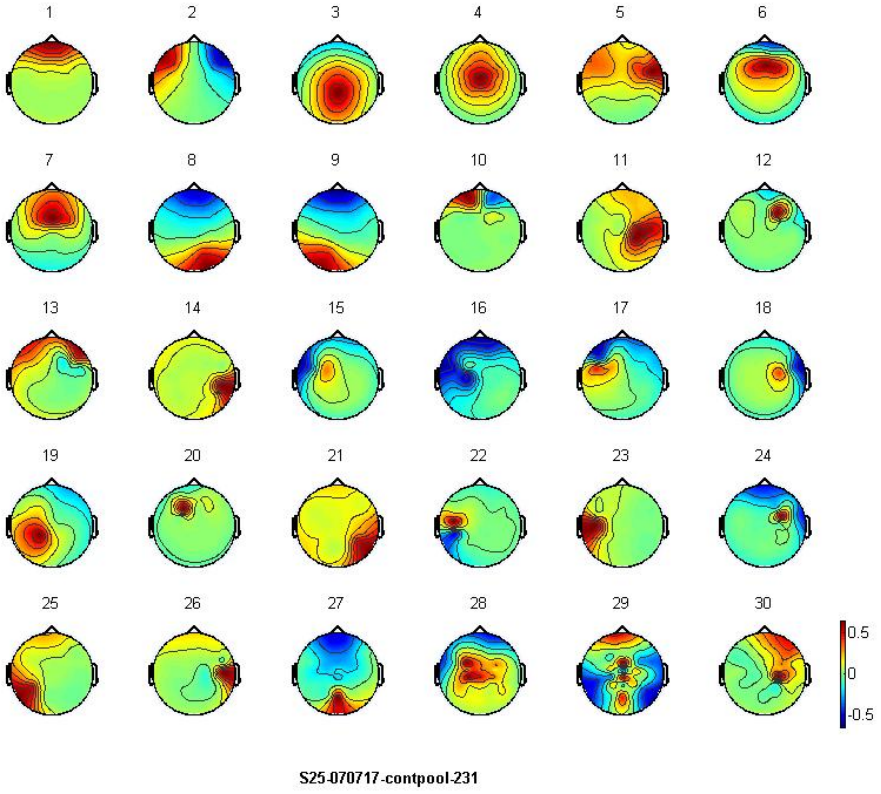

Figure 3-5: The picture shows the typical example of scalp topography of ICA decomposition of one subject. The scalp topographies show the ICA weighting matrix $\boldsymbol{W}$ projected to its corresponded component onto the surface of the scalp. A total of 30 components are separated from 30-channel EEG signals. The color bar indicated the amplitude of component signals

3.4 Event Related Spectral Perturbation (ERSP) Analysis

The ERSP, a kind of time-frequency analysis, which was first proposed by Makeig (Makeig, 1993), can reveal those time-locked but not necessary phase-lock event related activities. ERSP analysis transforms time-course signal into spectral-temporal domain. Therefore, activities of each frequency band associated

with navigation can be further analyzed. Fig. 3-7 illustrates an example of ERSP analysis of left motor component.

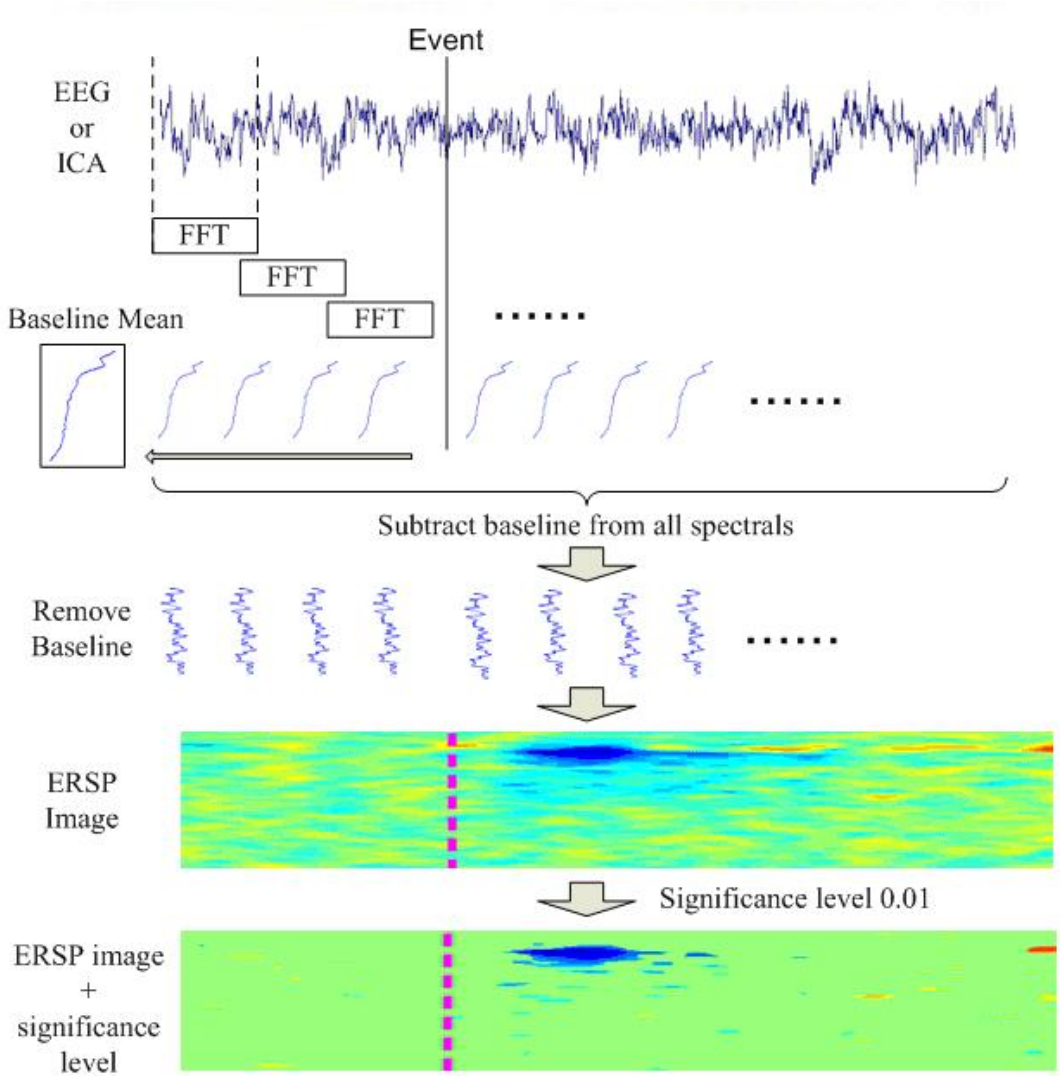

Figure 3-6: The picture shows the illustration of procedures in ERSP analysis. Short term FFT is applied in each window with 256 sample points, and overlaps by 244 sample points. In the final step, non-significant parts of ERSP image are set to zero by the means of bootstrap.

The processing flow was shown in Fig. 3-6. ICA activation was first divided into 200 512-point windows. Each window was multiplied with Hanning gain and then extended to 1024 points by zero-padding to calculate its power spectrum fast Fourier transform (FFT). Log power spectra were computed and then were normalized by

subtracting the baseline (straight tunnel segment) log mean power spectral. This procedure was applied to all the epochs. Time series of IC in each trial were transformed into time-frequency matrix (200 x 1024) with a frequency resolution about 0.05 Hz the results were then averaged to yield ERSP image. Fig. 3-7 gave an example of ERSP image which is motor component. Significance of deviations from power spectral baseline was assessed by bootstrapping, a nonparametric permutation-based statistical method. Non-significant points were masked as zero; only significant ($p<0.05$) perturbations were remained. Through ERSP, we investigated the time-frequency information of brain activity in different area during the tunnel task.

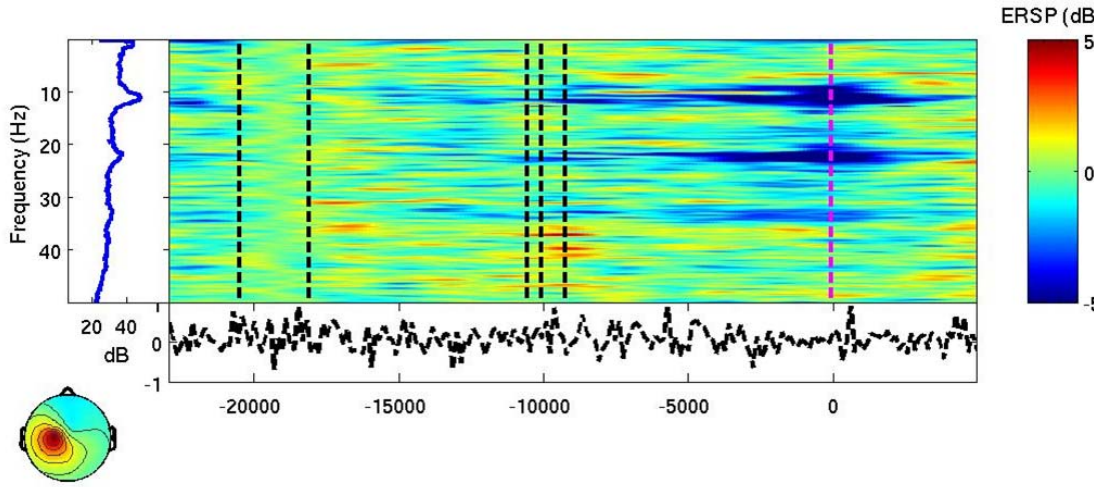

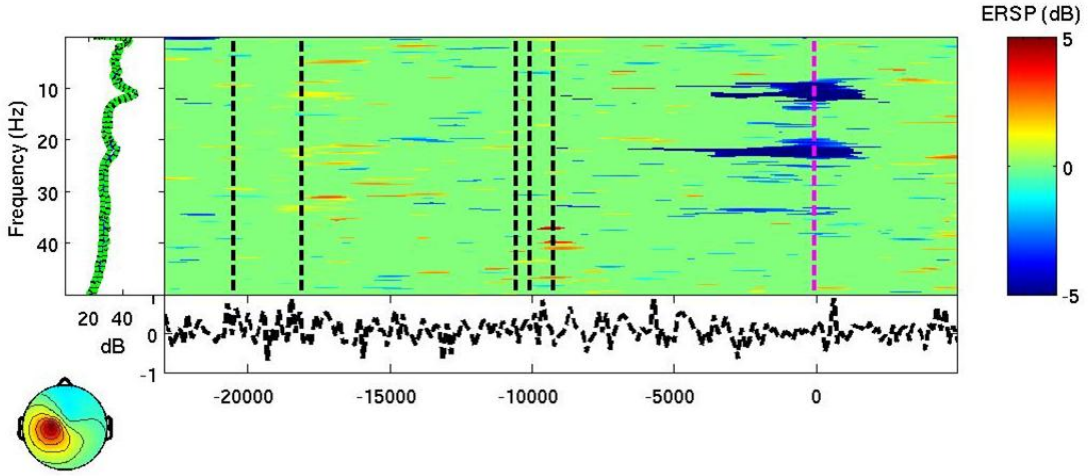

Figure 3-7: Pictures show the illustration of ERSP images of the left somatomotor component. (A): ERSP images of the left somatomotor component which do not mask by significance level. Note: the powers at around 10- and 20- Hz frequency bands shows apparently suppressed during the selecting homing angle period in comparison to the baseline period. Pink dashed lines: the averaged onset of forthright. Blue dashed lines: the mean onset of meander. Red dashed lines: the averaged response time of the homing direction selections. Black dashed lines: the mean response time of the homing angle selections. Color bars showed the power magnitude of ERSPs. (B) The same ERSP images shows in (A) but masks by significance level. The significance level was set at $p<0.05$.

3.6 Component Clustering

To compare electrophysiological results across subjects, the usual practice of most researchers has been to identify scalp channels. Component clustering would be used to assess the consistency of ICA decompositions across subjects and sessions, and to evaluate the separate contributions of identified clusters of these data components to the recorded EEG dynamics.

ICA components from multiple subjects and sessions were clustered semi-automatically based on their gradient of scalp projections, EEG characteristic and equivalent dipole location. These criteria for each IC were measured and compressed into 10-dimensional feature direction by principal component analysis (PCA). Semi-auto K-means algorithm was used to group similar ICs together and the clustering result was finally adjusted according to the time-frequency property and equivalent dipole location of each IC. The grand mean scalp map and spectra property were then computed for each cluster to investigate the common characteristics brain activity in the task. The process of clustering was shown as Fig. 3-8. Further analysis will base on the clustering result.

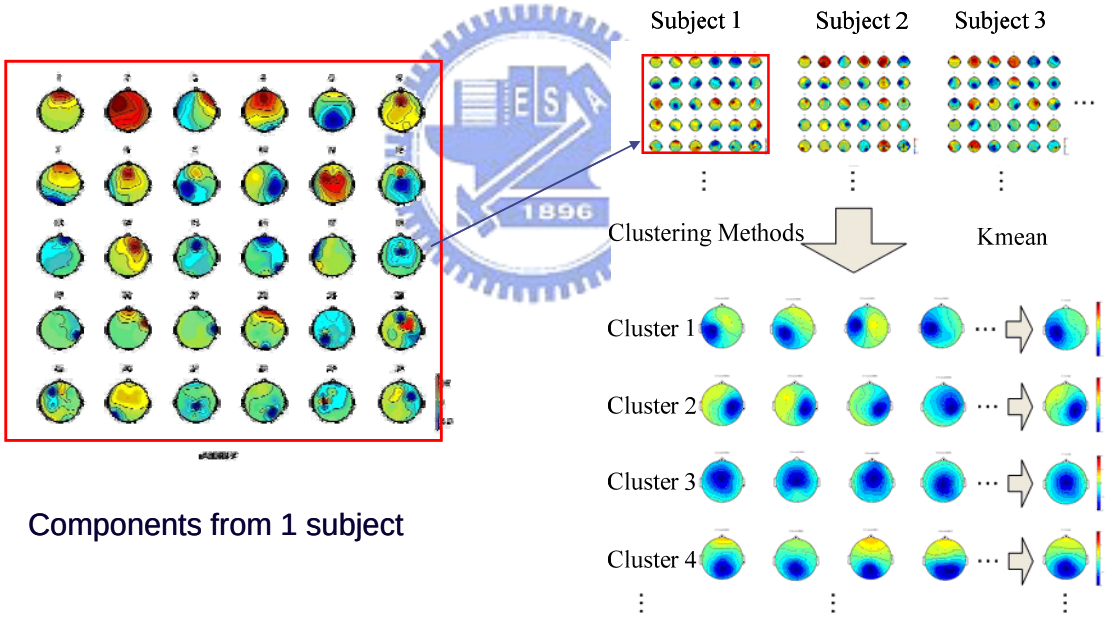

Figure 3-8: The picture shows the flowchart of component clustering analysis using the K-means algorithm. Brain process associated independent components (ICs) across subjects and sessions are first selected by observations according to theirs scalp map distribution and spectral property. Then, the selected ICs are semi-automatically clustered by Kmeans algorithm into several clusters which had similar EEG

characteristics. These clusters represent the activities from different brain areas, such as parietal, occipital, left somatomotor and right somatomotor area.

Chapter 4 Result

A total of 20 subjects completely finished this experiment; 11 of them were categorized into allocentric subjects, and 7 participants were categorized into egocentric subjects. The rest three subjects' were not able to be classified into any category because their homing direction selections varied trials by trials. The influences of the choice of reference frame during the navigation on subjects' behavioral performance were presented in the first section. Then, the characteristic neural activities among the different brain regions in these two groups were presented in the second section and the last section presented differences on the brain oscillations in the parietal and the occipital regions between these two types of subjects in terms of the baseline and phasic power spectra as well as the ERSPs.

4.1 Behavioral Performance

The mean response time for determining the homing direction of 6 groups were ranged from 550 to 650 msec (Fig. 4-1). No apparent differences reflected on distributions of the response time of the homing directional selection between the allocentric and egocentric subjects [$F(1,2256) = 0.2324$; $p = 0.79265 > 0.05$]. Similarly, the turning degree did not have any influences on the speed of the homing directional selections [$F(2, 2256) = 0.8768$; $p = 0.34918 > 0.05$]. No interactions were found between the factors of strategy and turn eccentricity [$F(2, 2256) = 0.56369$; $p = 0.56918 > 0.05$].

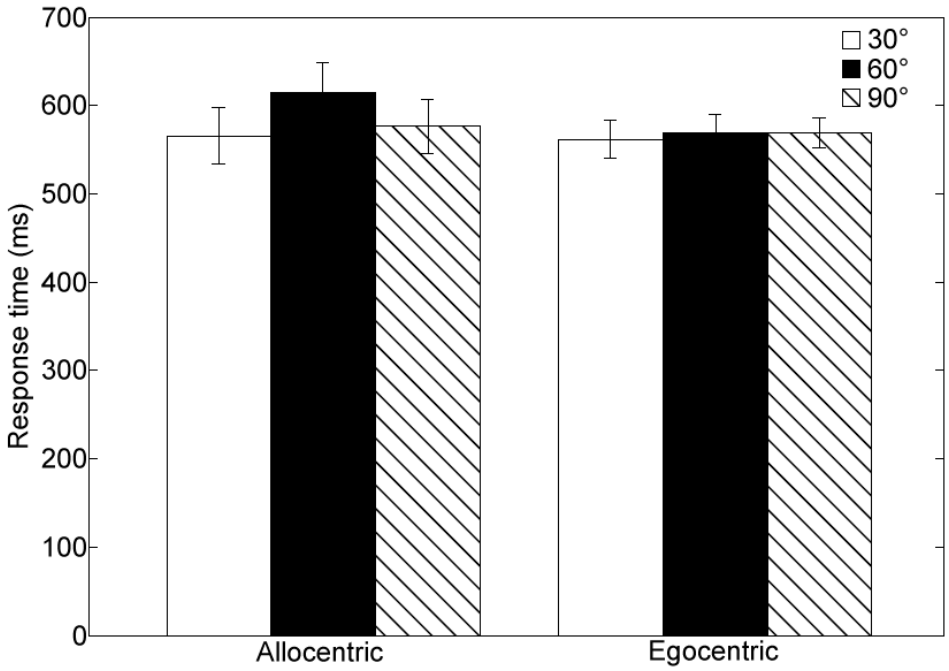

Figure 4-1: Effects of the navigation strategy and the turning degree on the grand mean of the response time for determining homing directions. Note no differences in the distribution of the response time are observed among 6 different groups.

Effects of the navigation strategy and the turning degree on the angle fit are showed in Fig. 4-2. The average absolute errors of the homing direction were lower than 15° for the tuner and non-tuner subjects in three different turn angle. To further test the significance of effects on turning degree and the navigation strategy, we use 2 x 3 repeated-measures ANOVA. Results showed both the navigation strategy and turn angles have significant influences on the absolute errors of the angle fit [navigation strategy: $F(1, 2256)=98.993$; $p < 0.001$; turning degree: $F(2, 2256)=457.865$; $p < 0.001$), but no interactions were found between the two factors [$F(2, 2256)=0.876$; $p >0.05$]. For the allocentric reference frame users, the correctness for pointing the homing direction were decreased with the increases of the turn angle but such sequential drop on the response accuracy along with the increases of the turn angles did not reveal in the egocentric reference frame users. Specifically, the response

accuracy were as 60° > 30°> 90°. Comparing with the allocentric reference frame users, the response accuracy were significant higher for the egocentric reference frame users when turn angles were larger (60°: 7.52 ± 0.29 < 8.22 ± 0.22, p<0.005; 90°: 11.06 ± 0.37 < 14.32 ± 0.41, p<0.000) but their response accuracy were significant lower when the turn angles were small (30°: 5.39 ± 0.19 < 9.45 ± 0.30, p<0.000). The mean pointing errors for the egocentric reference frame users revealed that both the two reference frame users were easily to overestimate the homing direction when the turn angles were small (30°) while they were tend to underestimate the homing direction when the turn angles were larger (60° and 90°, Fig. 4-2B).

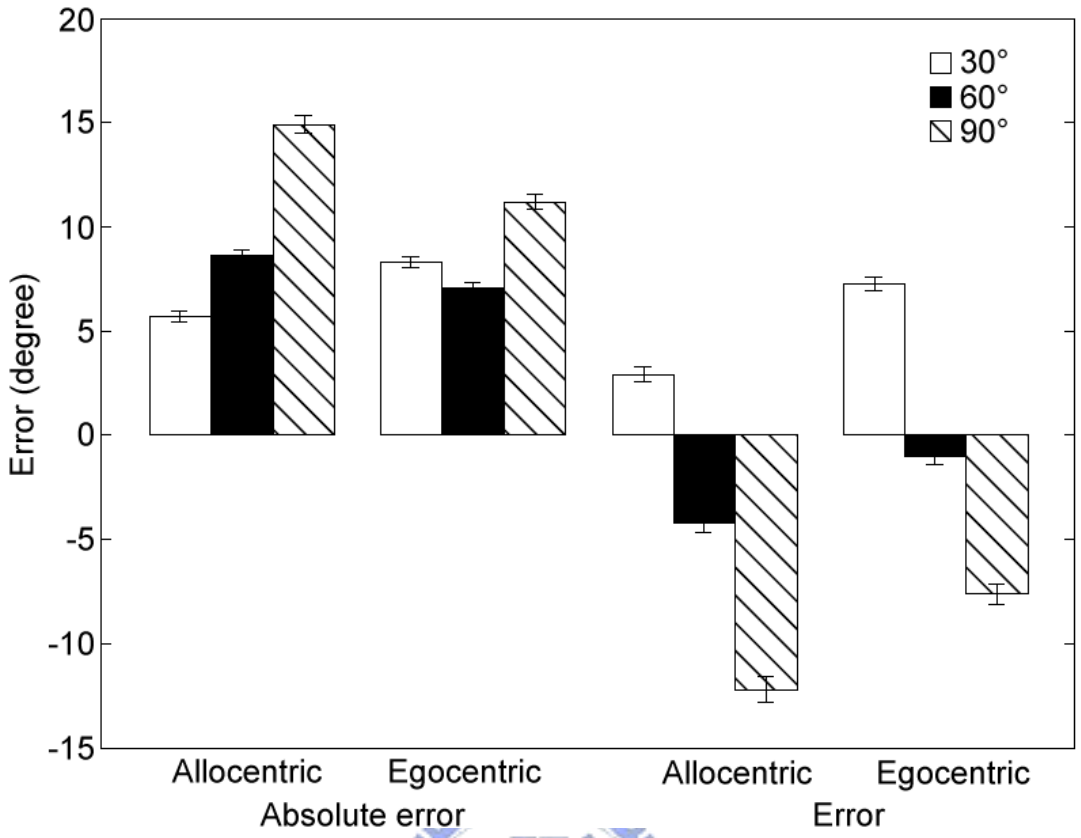

Figure 4-2: effects of navigation strategy and the turning degree on the behavioral performances which evaluated by the absolute error (A) or error (B) of the homing direction. Note: all the mean absolute errors were ranged from 5 to 15 degrees. A two way ANOVA test showed significant differences in the absolute error on factors of navigation strategies and turning eccentricity. The mean absolute errors indicate that subjects were overestimated the homing direction when the turn angles were small while the subjects were tended to underestimate the homing direction when the turn angles were larger.

4.2 Independent Component (IC) Clustering and Source

Localization

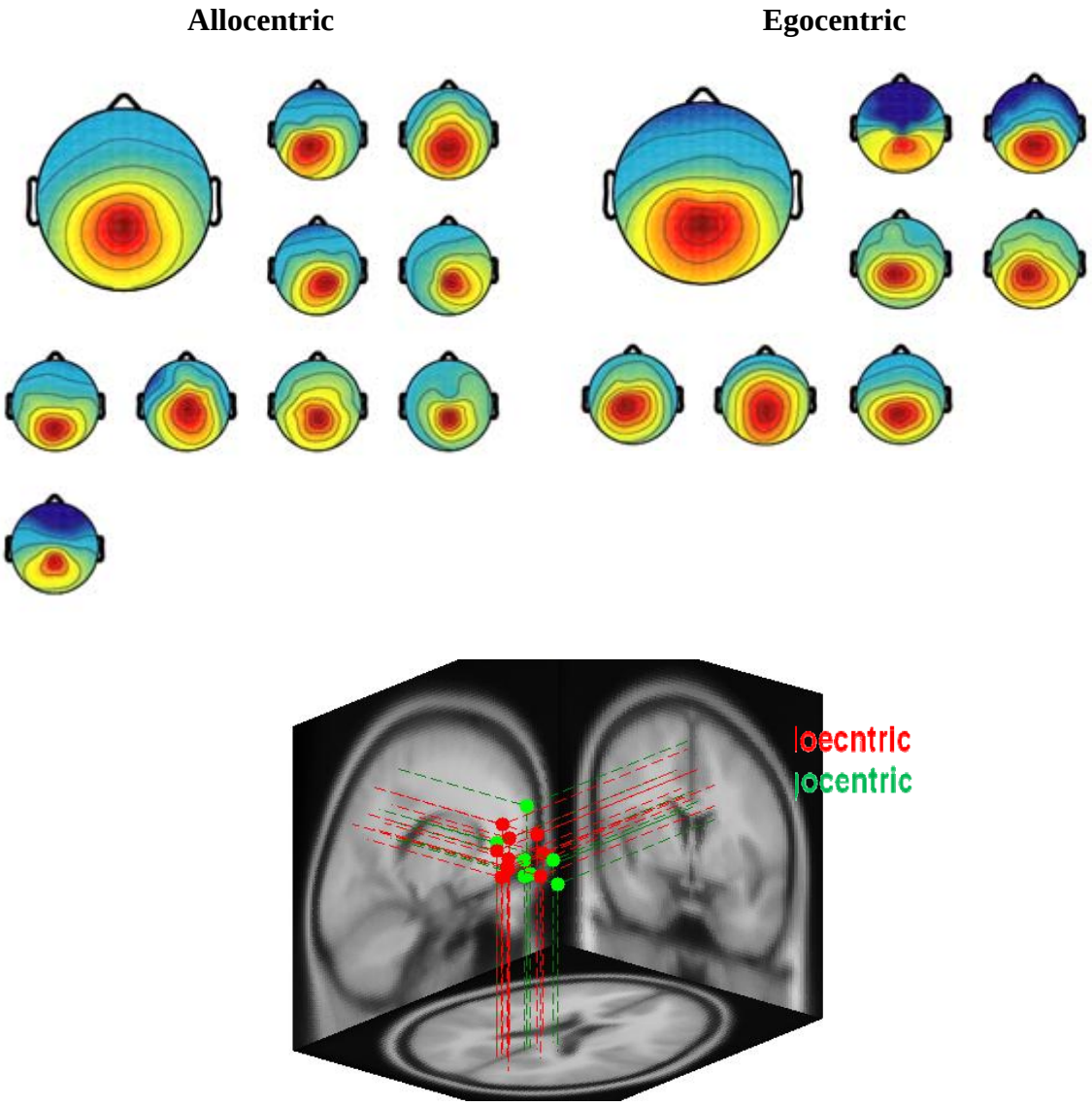

Figure 4-3: The grand mean of the scalp map and individual scalp maps (A, B) as well as their equivalent dipole locations (C) for the parietal IC clusters for the allocentric and egocentric subjects. A total of nine from 10 allocentric subjects exhibit parietal components, and 7 of 7 egocentric subjects exhibited parietal component.

Allocentric **Egocentric**

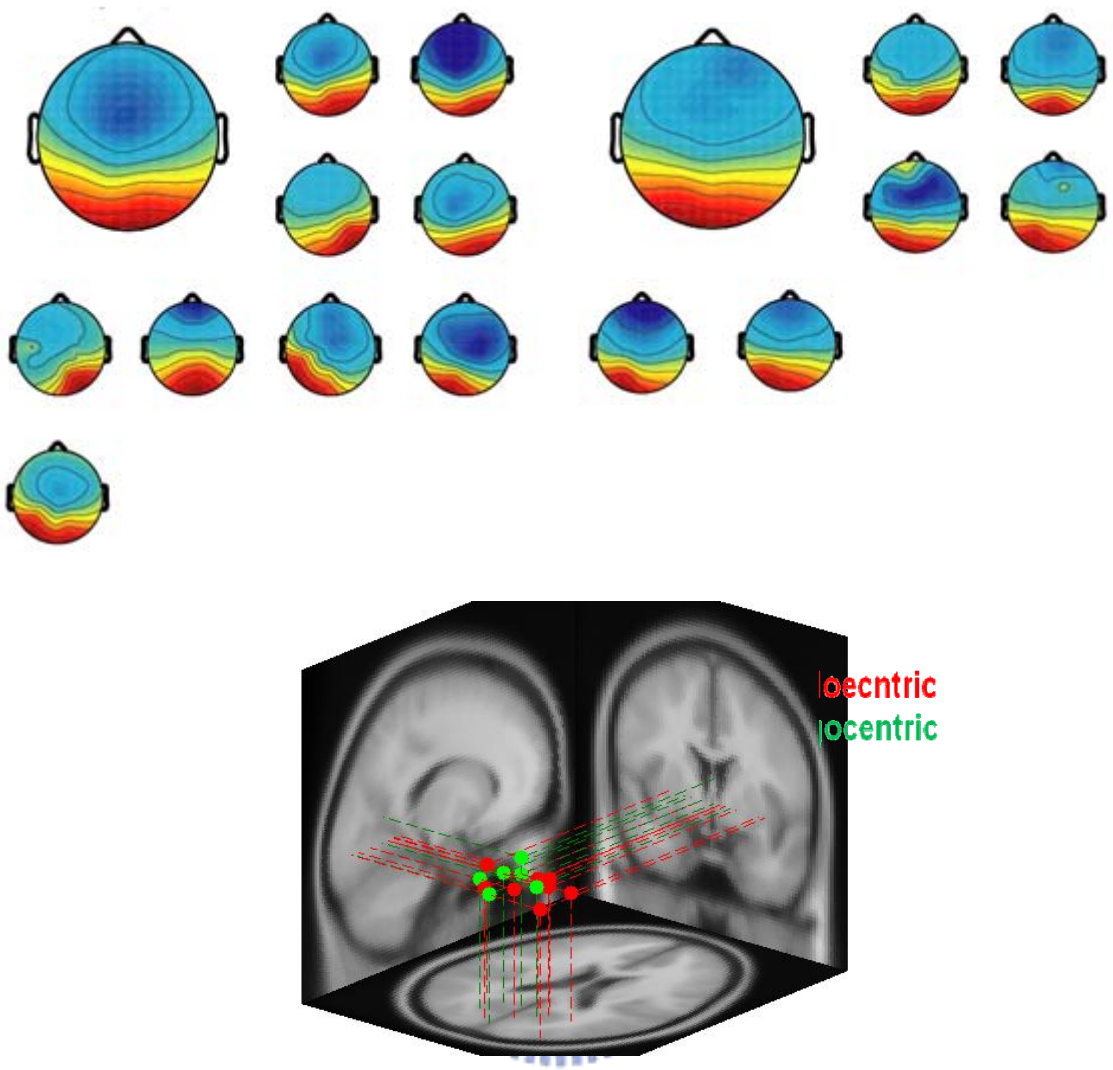

Figure 4-4: The grand mean of the scalp map and individual scalp maps (A, B) as well as their equivalent dipole locations (C) for the occipital IC clusters for the allocentric and egocentric subjects. Panels as Fig. 4-2. 90.0% (9/10) allocentric and 85.7% (6/7) egocentric subjects have occipital ICs.

Allocentric **Egocentric**

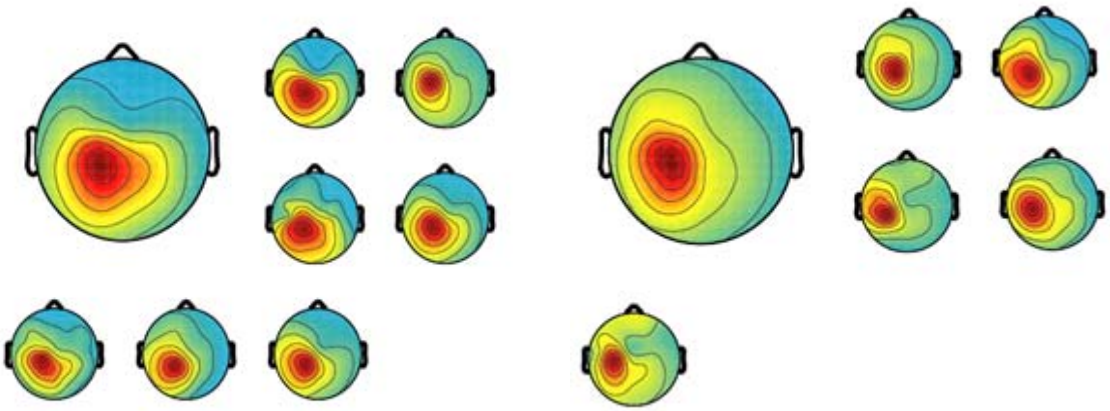

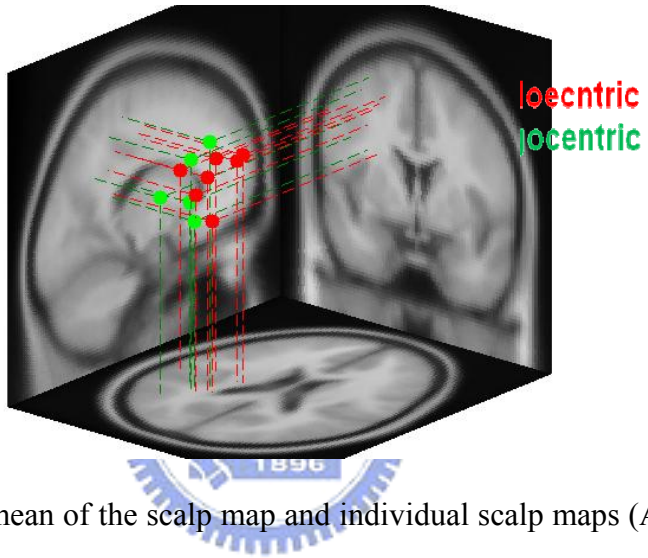

Figure 4-5: The grand mean of the scalp map and individual scalp maps (A, B) as well as their equivalent dipole locations (C) for the left somatomotor IC clusters for the allocentric and egocentric subjects. Panels as Fig. 4-2. 70.0% (7/10) allocentric and 71.4% (5/7) egocentric subjects are with the left somatomotor ICs

Results of the component clusters showed that the spatial navigation at least involved several brain regions. The number of localizable brain ICs in allocentric and egocentric reference frame subjects did not differ significantly [$F(1,2) = 0.05$, $p>0.05$, n.s.]. Neither did the numbers of ICs contributed by allocentric and egocentric reference frame subjects to the 3 clusters differ significantly [group by cluster interaction $F(2,2) = 1$; $p>0.05$, n.s.]. Fig. 4-3, 4-4 and 4-5 shows the grand mean of the scalp map, the scalp maps from individual subjects and their equivalent dipole

models for three major IC clusters (parietal, left somatomotor and occipital clusters) across 10 allocentric and 7 egocentric reference frame subjects. The residual variances and Talairach coordinates of the equivalent dipole sources and the numbers of independent components were summarized in table-1 and table-2, respectively.

Table-1: The residual variances and Talairach coordinates of the equivalent dipole sources

Component	*Residual variance (%)*	*Talairach coordinates*			*Distance to cluster center (nm)*
		x	y	z	
Parietal Cluster					
S09-070508	1.54%	-25	11	36	14.4
S10-070502	1.85%	-29	7	28	9.6
S11-070508	1.27%	-29	-17	24	18.3
S13-070511	3.31%	-41	3	36	10.3
S16-070523	1.11%	-37	-1	28	6.5
S20-070613	5.41%	-5	7	24	29.5
S23-070709	4.63%	-57	-17	36	29.7
S24-070710	4.33%	-41	-1	24	12.1
S26-070730	3.15%	-37	3	48	16.8
S28-070820	3.23%	-21	-5	40	14.1
mean	2.98%	-32.2	-1	32.4	
S17-070531	6.42%	11	-5	8	31.4
S17-070531	6.46%	-9	-5	24	30.1
S18-070606	2.53%	-21	-1	20	24.6
S19-070606	3.41%	-21	3	52	56.1
S21-070704	1.72%	-33	11	36	43.8
S22-070705	1.96%	-25	-1	28	33.2
mean	2.64%	-17	3	-4	
Occipital Cluster					
S09-070508	1.80%	-33	-17	-4	24.3
S10-070502	1.23%	-25	-9	-4	16.4
S11-070508	3.03%	-33	-33	-4	40.1
S13-070511	2.97%	-45	-5	-4	20.0
S20-070613	8.31%	-57	-37	-4	52.1
S23-070709	1.79%	-29	-5	-4	12.0
S24-070710	5.15%	-29	31	-4	24. 0
S26-070730	2.44%	-53	7	-4	24.0
mean	6.08%	-29	7	-4	
S17-070531	4.19%	-37	-13	-4	17.6
S18-070606	0.70%	-57	-1	-4	18.2
S19-070606	15.48%	-37	-1	8	11.6
S21-070704	6.08%	-45	19	-4	15.7
S22-070705	2.41%	-33	15	-4	12.7

S27-070809	1.98%	-29	7	-4	11.1
mean	5.14%	-39.67	4.33	-2	
Left Motor Cluster					
S11-070508	2.55%	-5	23	44	19.4
S13-070511	0.43%	-1	47	36	23.1
S20-070613	5.44%	-21	27	16	16.0
S23-070709	2.17%	-5	27	40	15.5
S24-070710	2.78%	-21	31	36	6.4
S26-070730	1.15%	-41	27	16	28.5
S28-070820	1.61%	-25	35	28	9.4
mean	2.30%	-17	31	31	
S17-070531	1.65%	-37	47	28	16.6
S19-070606	2.56%	-25	39	44	12.0
S21-070704	6.09%	-5	43	56	28.6
S22-070705	1.92%	-17	47	20	14.4
S25-070717	3.29%	-25	35	16	18.5
mean	3.10%	-21.8	42.2	32.8	

Table-2: The Number of Components in the three IC Clusters

	Parietal	**Occipital**	**Left Motor**	**Total**
Number of subjects (Allocentric)	90.0% (n=9)	90.0% (n=9)	70.0% (n=7)	25
Number of subjects (Egocentric)	100% (n=7)	85.7% (n=6)	71.4% (n=5)	18
Total	16	15	12	43

4.3 Brain Dynamics of the Allocentric representation

4.3.1 The Parietal Component

The Fig. 4-6 shows the grand mean of ERSP images of the parietal IC cluster across 9 subjects who used the allocentric reference frame in the experiment. Results revealed that the alpha band power and its first harmonics slightly attenuated while subjects passed through the curve, and the alpha band power was increased during and after homing direction selections. The above changes in alpha band power were

observed in all turning degree.

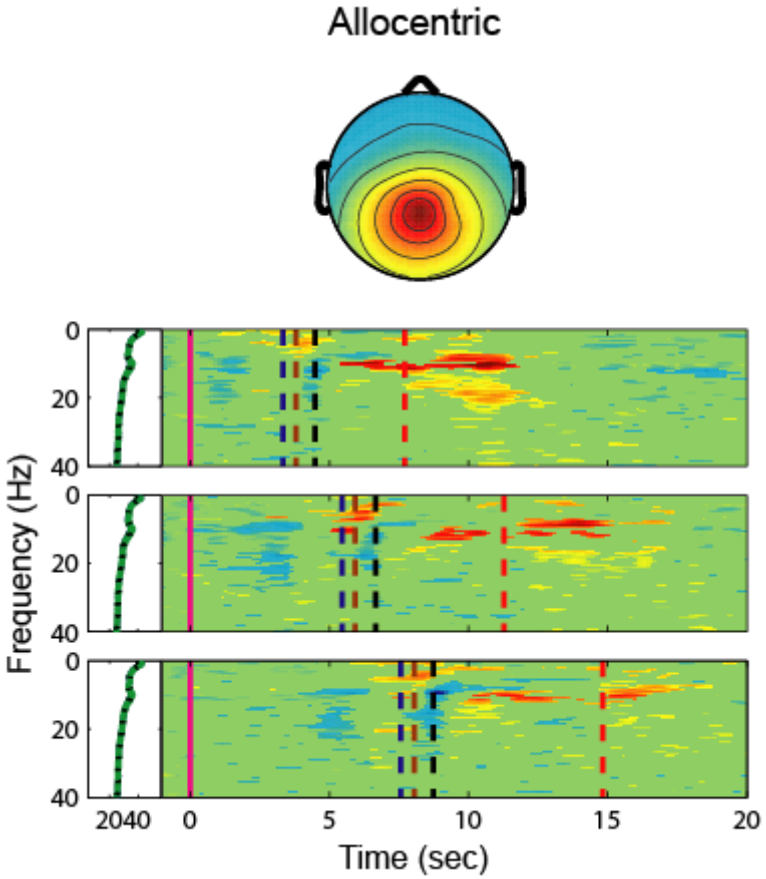

Figure 4-6: The grand mean of the ERSP images (lower panels) and the average component map (top panel) of the parietal cluster across 10 subjects used the allocentric reference frame. Epochs were aligned to the onset of entering the tunnel, and straight segment was selected as baseline. Solid pink lines: the onset of turn. Blue dash lines: the offset of the turn. Brown dash lines: the onset of exiting the tunnel. Black dash lines: the onset of selecting the homing direction. Red dash lines: the onset of selecting the homing angle. Note: the ERSP images showed that the alpha band power and its harmonics slightly decrease while passing through the curve, and then the alpha band power increases during and after selecting the homing angle. The above phenomena are observed in three cases which are with 30°, 60° and 90° turning angles respectively.

4.3.2 The Occipital Component

Figure 4-7 shows the grand mean of ERSP images of occipital IC cluster across 9 allocentric reference frame subjects. Results showed that the alpha band power slightly decreased when subjects passing through the tunnel turn. The alpha band power strongly increased before the end of turn and the increased alpha activity was sustained through the second straight segment and the homing directional selection. When subjects responded to the homing angle selection, the stronger and sustained power decrease in alpha band was appeared and followed by another alpha band increase beginning around 1 sec after the end of the homing direction selection. No apparent differences on the EEG dynamics were found in the occipital IC cluster among three cases, which were composed trials with different turning angles.

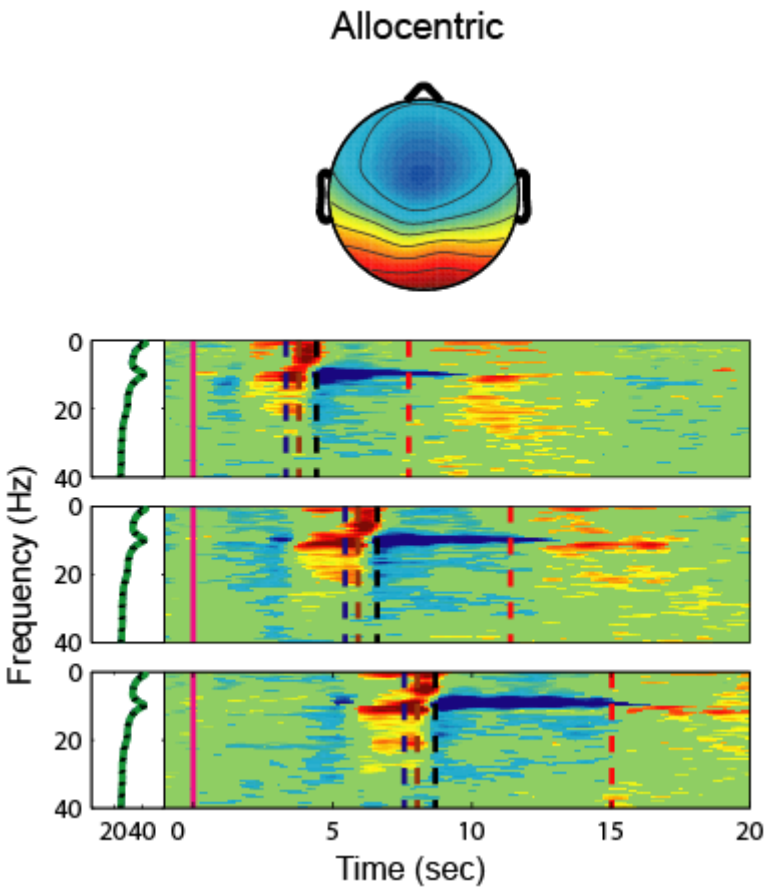

Figure 4-7: The grand mean of the ERSP images (lower panels) and the average component map (top panel) of the occipital cluster across allocentric subjects. Panels as Fig. 4-6. Note: the alpha band power slightly decreases when subjects passing through the curve segment while it increases strongly at the end of tunnel. Then, the alpha power suppresses strongly during the homing angle selection. Finally, the alpha power increases again after the end of the angle selection. The above phenomena are observed in all cases.

4.3.2 The Left Motor Component

To characterize the changes of the neural activities related to process homing angle decisions at the somatomotor IC cluster, all trials were aligned to the onset of the homing direction selection and shows in Fig. 4-8. A strong alpha/mu activity near 10 and 20 Hz suppressed from the end of the tunnel turn and sustained to the end of the homing directional selection. Following the alpha blocking, an increase in alpha

band activity showed after the end of the homing direction selection. In comparison to the cases with larger turning angles (60° and 90°), a power increases in the beta band (roughly around the 20 Hz) clear presented in the case with the small turning angle (30°) after the end of the homing direction selection. No additional apparent effects of the turning angle were found in the ERSP images of the IC clusters.

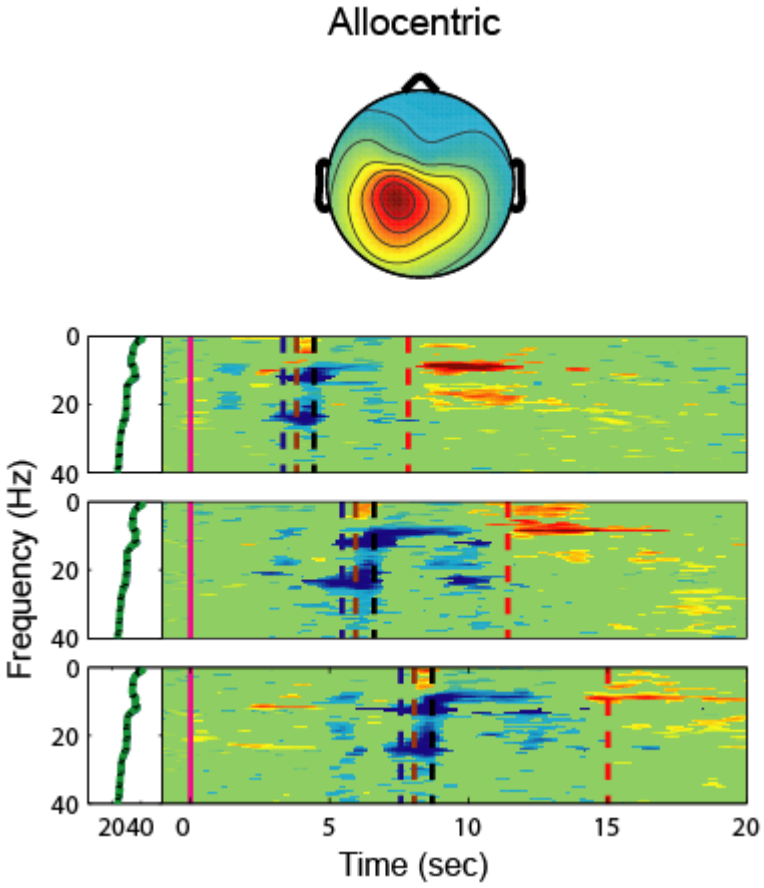

Figure 4-8: The grand mean of the ERSP images (lower panels) and the average component map (top panel) of the left somatomotor IC cluster across 7 allocentric subjects. All the traces were aligned to the onset of the homing direction selection. Panels as Fig. 4-6. Note: Strong alpha/mu activity was suppressed from the turn segment to the homing direction selection period. An increase in alpha activity was found after the end of homing direction selection.

4.4 Brain Dynamics of the Egocentric reference frame subjects

4.4.1 The Parietal IC clusters

The activities in alpha band and its harmonics were minor attenuated from around 1 to 3 sec after the entrance of the tunnel turn, and the higher alpha band power (around 10-12 Hz) sustain increased during the second straight segment and the period for determining the homing directions. After the end of the homing direction selection, the slightly increases in the beta band (around 14-30 Hz) apparently showed in the trails with 30° tunnel turns.

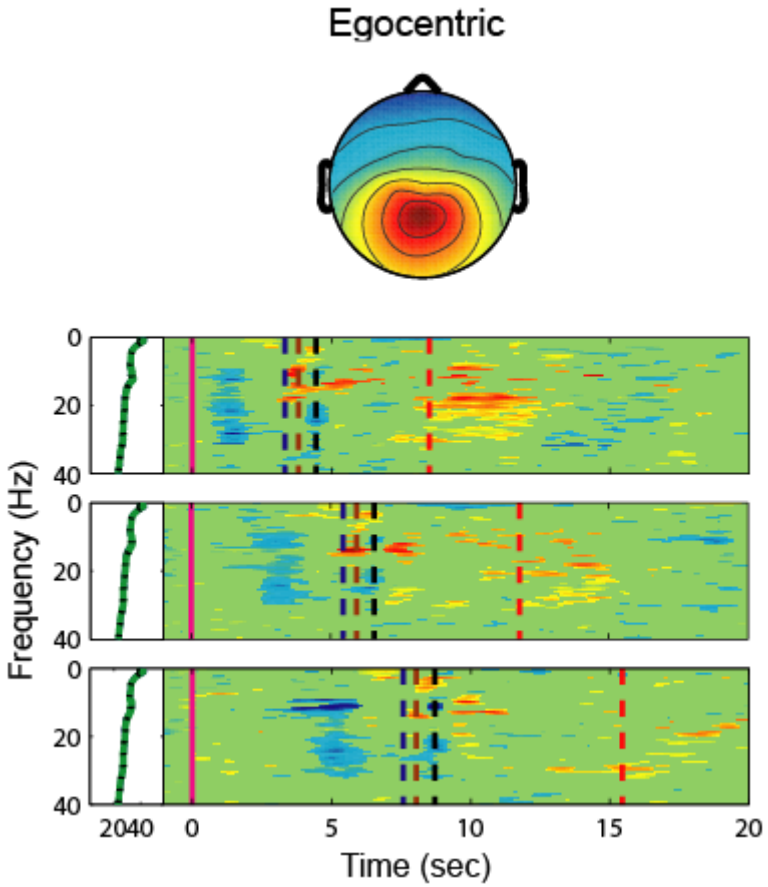

Figure 4-9: The grand mean of the ERSP images (lower panels) and the average component map (top panel) of the parietal cluster across egocentric subjects. Panels as Fig. 4-6. Note: Alpha band power and its harmonics attenuated while passing through the curve, and the alpha band power is increased while and after pointing the angle. The larger tunnel degree revealed stronger alpha attenuation while passing through the curve but weaker wide band enhancement after button press.

4.4.2 The Occipital IC cluster

In the occipital IC cluster, strong increases in alpha band and its harmonics revealed 2 sec before the end of the turn segment and through the second straight segment and the power increase downward shifted to around 4-8 Hz during the homing directional selection (Fig. 4-10). Following the onset of homing direction selection, the alpha band and its first harmonics powers decreased again and sustained

to the end of the button press. A short duration of power increases near 10 and 20 Hz showed around 2.5 sec after the button press.

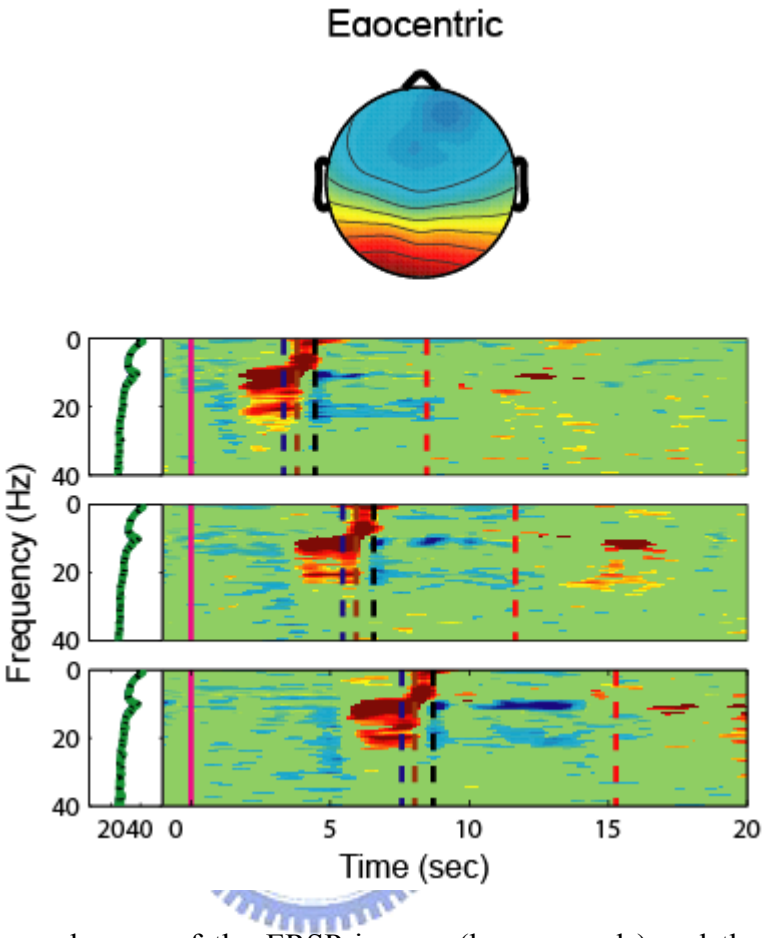

Figure 4-10: The grand mean of the ERSP images (lower panels) and the average component map (top panel) of the occipital cluster across egocentric subjects. Panels as Fig. 4-6. Note: We found strong alpha band power increased in the end of tunnel and alpha attenuation while subjects were pointing the homing angle consists in all tunnel cases.

4.4.3 The Left somatomotor IC cluster

The alpha/mu suppression showed from passing though the second straight segment of the tunnel and the homing degree and direction selection (Fig. 4-11). The clear power increases in the alpha/mu rhythms were only found in the trials with 60° turn angles. The observed phenomena were similar to those found in the allocentric

reference frame subjects. Science phenomena of the right somatomotor IC cluster was similar with left somatomotor IC cluster, therefore we showed left somatomotor IC cluster only.

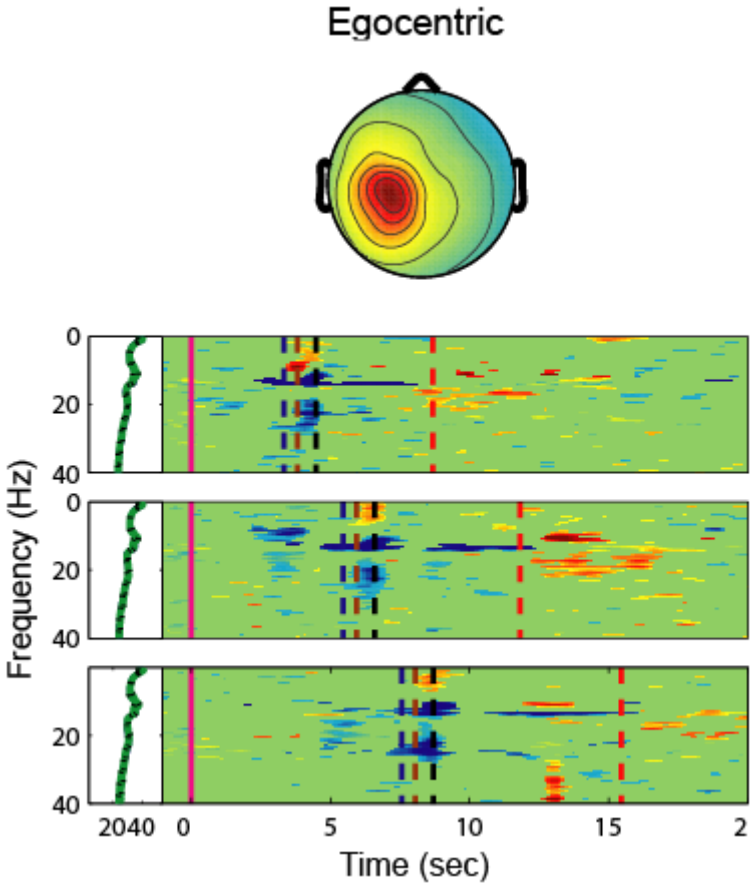

Figure 4-11: The grand mean of the ERSP images (lower panels) and the average component map (top panel) of the occipital cluster across egocentric subjects. Panels as Fig. 4-6. Note: Strong mu rhythm suppression showed from passing though the second straight segment of the tunnel and the homing directional and direction selection, then the increase activity in alpha band revealed around 1 sec after button press.

4.5 EEG differences between two strategy groups

To study the possible group differences in EEG activities more closely, we assessed the tonic power changes in EEG spectra of the three major IC clusters

between the two groups and the significance of those differences between the two groups were further confirmed by repeated-measures ANOVA.

Figure 4-12 shows the tonic and phasic changes in power spectra of the parietal IC clusters for two groups. The peak of the baseline power spectrum of the allocentric reference subjects was around 10 Hz while egocentric reference frame subjects exhibited the peak around 12 Hz. In comparison with the egocentric reference frame subjects, the baseline power of the subjects using the allocentric reference frames, were significant higher at the frequencies around 4Hz, 8-12Hz, 16-20 Hz and 36-40Hz. The above differences between these two strategy groups were not affected by the turning degree. The similar differences on the baseline power spectra between the two groups also revealed on the distribution of their phasic power spectra, but such differences did not reach the statistic significance. The occipital IC cluster also showed the significance difference on the peak of the baseline power spectra between the two types of subjects (Fig. 4-13). The baseline powers were significant higher at the frequencies at 8-11 Hz.

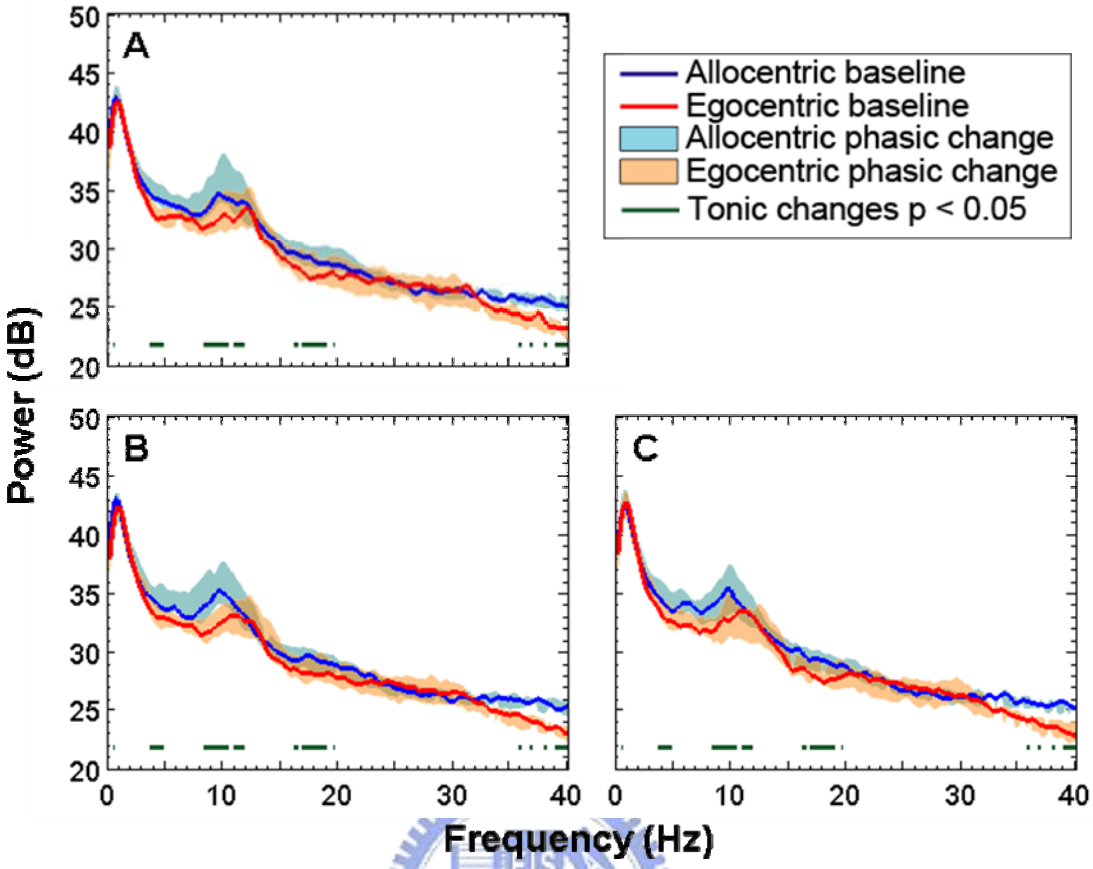

Figure 4-12: The averaged power spectral changes in tonic and phasic responses in parietal component. Turning angles are degrees of 30 (A), 60 (B), and 90 (C) respectively. Blue and red lines: mean spectral power of baselines for allocentric and egocentric subjects respectively. Light blue shadow marks the maximal and minimal of the phasic changes in the power spectra for the allocentric subjects. Light red shadow marks the maximal and minimal of the phasic changes in the power spectra for the egocentric subjects. Green horizontal lines mark the frequency ranges where the tonic power spectra are significantly different ($p < 0.05$) between allocentric and egocentric subjects. Note: for the allocentric subjects, the peak of the spectra is located at the low alpha band while it is located in the high alpha band for the egocentric subjects.

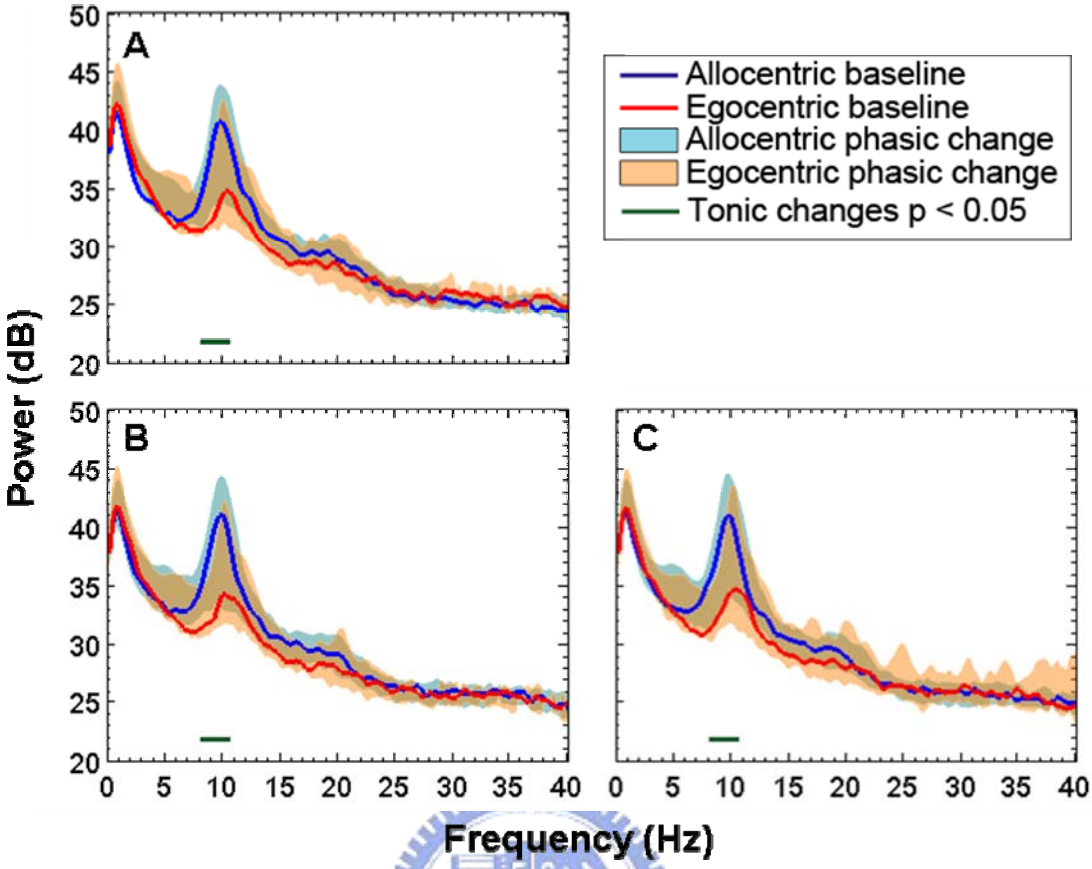

Figure 4-13: The averaged power spectra of the tonic and phasic responses in occipital IC clusters for allocentric and egocentric reference frame users. Panels as Fig. 4-12. Note: the peaks of the spectra are located near 10 Hz for both allocentric and egocentric subjects. Comparing with the egocentric reference frame subjects, the tonic power of subjects using the allocentric reference frame were significantly higher at the frequencies around 10-11 Hz ($p < 0.05$, mark in green horizontal line).

To further assess the relationship between the changes of the brain activities and the navigation performances, we further grouped the trials by their navigation performance and classified as the good estimation, under estimation and over estimation groups and redrew the ERSP images of these three groups. Results demonstrated that the navigation performance related changes on brain activities were in the parietal IC cluster of the egocentric reference frame subjects (see Fig. 4-14). Comparing to trails with well-estimation of homing angle, the power attenuation at

the frequencies at 8-30 Hz (around alpha and beta band) was stronger when subjects overestimated homing directions, but the attenuation power was decreased when subjects were underestimated the homing directions. The Fig. 4-15 shows the quantitative comparisons of the performance related variations on parietal IC cluster activities.

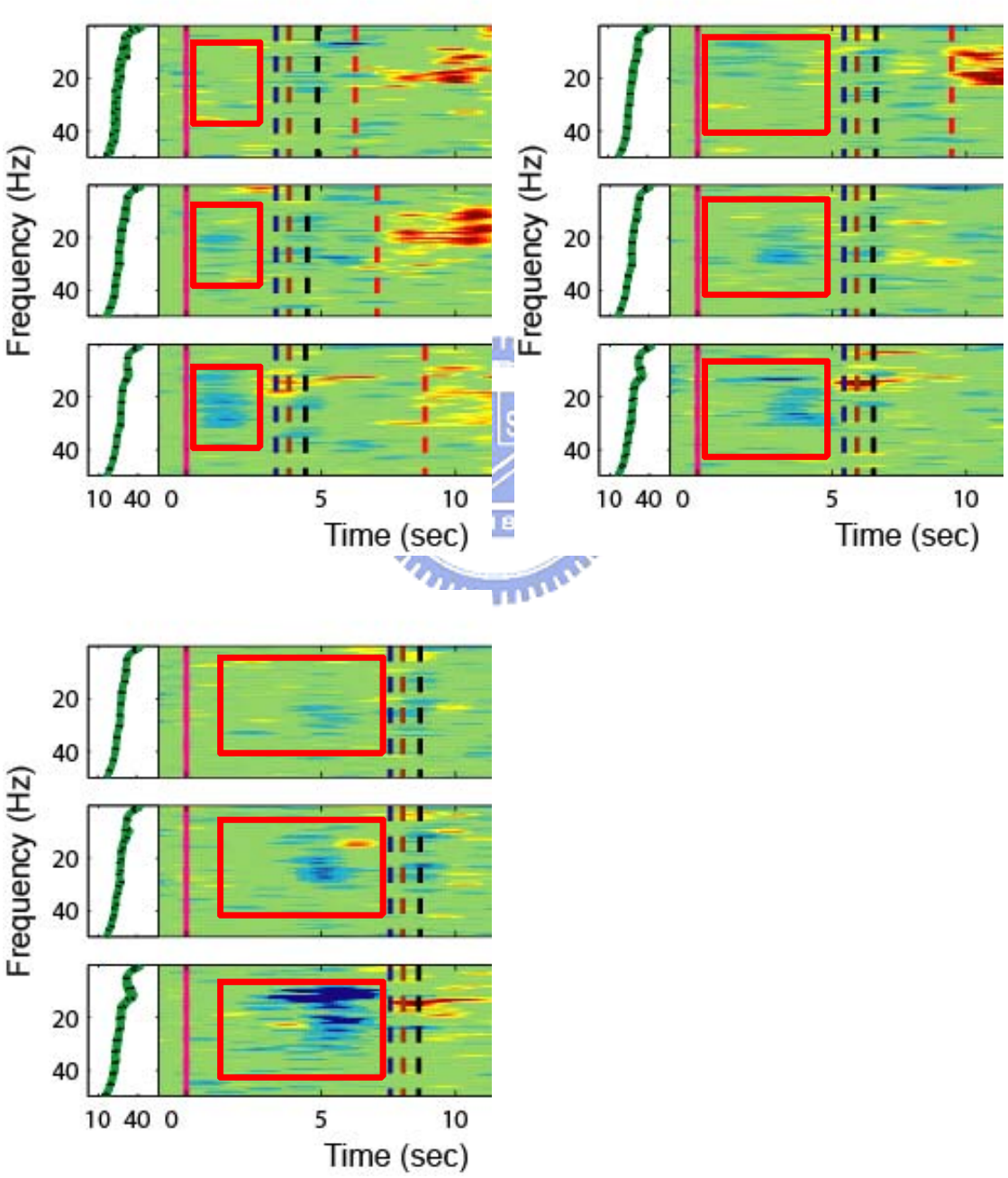

Figure 4-14: Performance related parietal EEG activities. Upper panels: parietal ERSP

image of egocentric subjects of trails with under-estimated homing angle. Middle panels: parietal ERSP image of egocentric subject of trails with well-estimated homing angle. Lower panels: parietal ERSP image of egocentric subject of trails with over-estimated homing angle. The turn angles were (A) 30°(B) 60° and (C) 90°, respectively. Since the duration of tunnel passage is less than 10 sec, ERSP images here only showed the changes at the first 10 sec of the trails. Note: When subject overestimated the homing directions, frequencies from 8 to 30 Hz were stronger suppressed during the tunnel passage. In contrast, the power attenuation was apparently less when the subjects underestimated the homing directions.

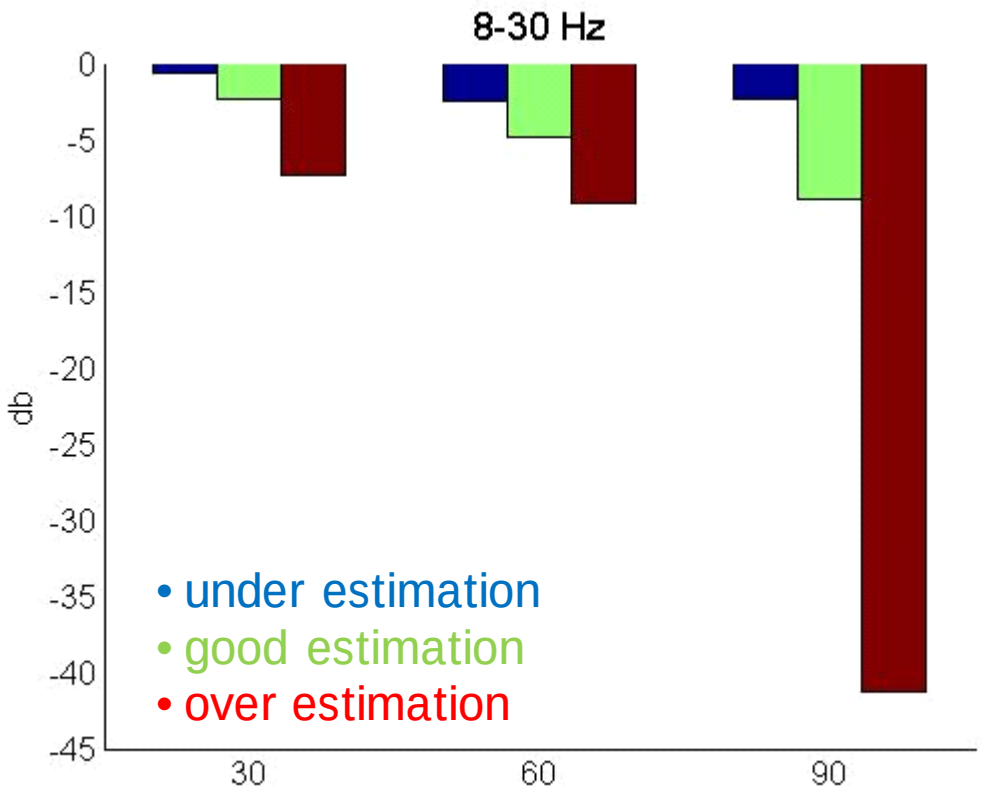

Figure 4-15: Bar chart of attenuated power summation with the frequencies at 8-30 Hz when the egocentric reference frame subjects passing through the turn segment of the tunnel. In comparison with the good estimation trials, the total power of overestimated trials was lower while the total power of underestimated trials was stronger. Furthermore, the turning degree enhanced the above differences.

Chapter 5 Discussion

In this study, we investigated the differences of brain activation between subjects using the allocentric reference frames and subjects using the egocentric reference frames during spatial navigation. Results showed that the navigation strategy do not have an apparent effect on behavioral performance in this simple tunnel task. The EEG results showed the use of allocentric and egocentric reference frame during navigation involved in different brain activations in the parietal and occipital regions. Furthermore, the power changes at the frequencies around the alpha and beta bands were highly related the navigation performance, evaluated by errors of determining the homing direction, in the subjects using egocentric reference frame during passing the turn segment of the tunnel.

5.1 EEG dynamics associated with allocentric and egocentric representation

Results showed that many brain areas involved in spatial navigation processes and the phenomena of the consist activations in the parietal and occipital areas in during spatial navigation was plausible with their well-supported roles in visuospatial task. For example, the parietal lobe (Fig. 5-1) has known to play an important role in integrating sensory information coming from various parts of the body, particularly determining spatial sense and navigation (Blakemore and U. Frith, 2005). The occipital lobe which locates in the rearmost portion of the skull (Fig. 5-1) is the visual processing center of the human brain and is known can be broadly activated in visual tasks including color discrimination, motion perception, navigation, and even mental imagery (Kandel et al., 2000).

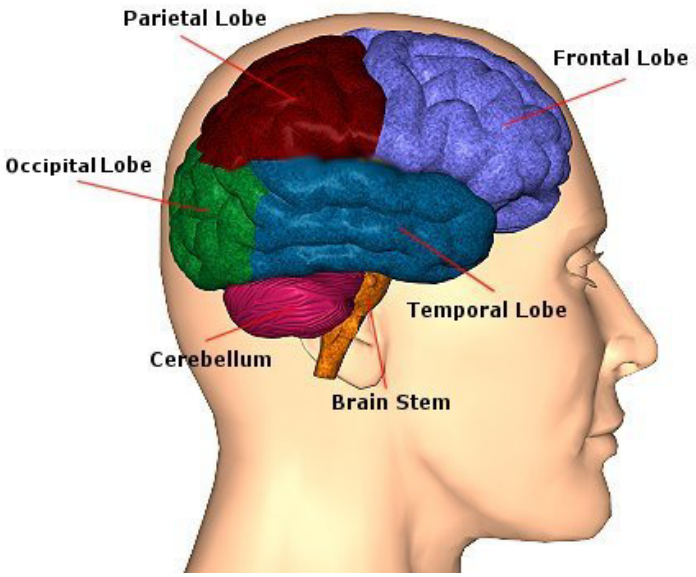

Figure 5-1: Location of the human brain lobes.

During tunnel passage, alpha suppressions associated with the path integration were found in both parietal and occipital area. Alpha suppression or event-related desynchronization (ERD) is well known for its relation to cortex activation (Pfurtscheller et al., 1996). The alpha suppression in occipital accompany with heading orientation may reflect activation of cortical to process the path integration visual flow information about rotation and translation during tunnel passage (Morrone et al., 2000; Kandel et al., 2000). The parallel alpha attenuation in the parietal area may involve in spatial awareness and processing of upcoming path information according to the dorsal pathway stretches from occipital lobe (Jong et al., 1994; Field et al., 2007). Subjects who used the allocentric reference frames showed stronger activation in occipital area comparison with the subjects using the egocentric reference frames. In contrast, subjects using the egocentric reference frames showed stronger activation in parietal during tunnel passage. The result is consistent with those neuron image studies which demonstrated that the tuners, using the egocentric reference frames, revealed stronger activation in parietal region during spatial navigation (Mellet et al., 2000; Galati et al., 2000; Committeri et al., 2004; Gramann

et al., 2006; Zaehle et al., 2007) whereas the subjects who used the allocentric reference frames activated a network comprising the parietal area and occipito-temporal area.

The alpha band power increased in parietal and decreased in occipital during deciding the homing direction and such alpha band power enhancement was thought to be an index of cortical inactivity (Pfurtscheller et al., 1996; Lin et al., 2005) or related to internally driven mental operations (Cooper et al., 2003, 2006; Klimesch et al., 2007). Since subjects had keep attention to the turning arrow and tried to recall the homing direction, the increased alpha power in the parietal area is not simply due to the cortical idling, but it may be an active processing which is necessary for internally commutating reference frames. Similarly, subjects who use an allocentric reference frame showed stronger alpha attenuation in occipital area during the homing direction selections. The task related alpha suppression in the occipital may not only reflect the process of visual information, but may also involve in the internal process of reference frame.

Results also revealed the different phasic power changes on EEG dynamics between allocentric and egocentric subject. The different tonic power changes on the theta, alpha, and beta band were showed in parietal area while only alpha band powers showed the different in occipital area between the two navigation strategy subjects. The theta oscillatory has thought to encode the spatial representation. Specifically, Nishiyama and Yamaguchi (Nishiyama et al., 2002) showed that theta activity over frontal and parietal-temporal regions were associated with learning maze navigation and they also suggested that theta activity could reflect connections between hippocampus and frontal, parietal cortex. The significant differences on tonic power changes at several frequency band indicated that the parietal as well occipital regions

played different roles between two navigation strategy subjects.

In the left somatomotor ICs clusters, both allocentric and egocentric subjects revealed sustained alpha and its first harmonic suppression, also called mu suppression during tunnel passage and selecting homing angles. Mu rhythm is strongly suppressed during the performance of a motor action or intentional movements (Salmelin and Hari, 1994; Pfurtscheller et al., 1996; Pineda, 2005). During tunnel passage, subject could percept the perspective visual flow of motion and then required to press button for answering direction and therefore the mu blocking showed in this area was expectable.

5.2 EEG Dynamics associated with navigation performance

Relationship between the brain activity and navigation performance was first demonstrated in this study. Comparing to trails with well-estimation of homing angle, parietal EEG activities of subject who use egocentric representation at the frequencies from 8 to 30 Hz were consistently stronger attenuated when subject overestimated homing angle. Oppositely, when subject underestimated homing angle, the EEG power at the same frequencies range were consistently less attenuated. The egocentric representation has suggested to involve the dorsal pathway (Sdoia et al., 2004; Committeri et al., 2004) which has also been reported relate to the accuracy of the predictions but not the content of subject's perceptual (Donner et al., 2007). Other researchers also found accuracy-predicted pre-stimulus brain activity (Makeig and Jung, 1996). Therefore this 8-30 EEG activity may be an index of navigation performance for egocentric subjects.

The hippocampus provides an allocentric representation of space and has found to associate with navigation performance. The higher accuracy of navigation was measured, the stronger activation of the right hippocampus was observed (Maguire et

al., 1998). Patients with hippocampal lesions also showed poor performance in large-scale complex environment navigation (Maguire et al., 2006). Brain activity in hippocampus is almost impossible to be detected from the scalp EEG due to its deep location in brain. Therefore, even though subjects who use an allocentric representation thought to involve visual -temporal pathway (Sdoia et al., 2004; Committeri et al., 2004), it is probably the reasons for explaining why we couldn't observe the specific performance related brain dynamics among occipital and temporal regions in the allocentric subjects.

Chapter 6 Conclusion

In this study, we investigated the differences of brain activation between the use of allocentric reference of frames and egocentric reference of frames in a tunnel navigation task. The tunnel task provides an elegant and sufficient way to separate subjects who preferred an allocentric or egocentric representation. Our result supported the dissociation brain activity between the uses of allo- and egocentric reference of frame. Subjects who prefer to use allocentric spatial representation showed stronger activation in occipital area during path integration while egocentric subject showed stronger activation in parietal area during path integration. The distinct brain regions involved in the navigation process may reflect that the encoding of allocentric and egocentric reference frames system are associated with ventral and dorsal neural networks streams respectively.

Reference

AD Ekstrom et al., 2003. Cellular networks underlying human spatial navigation. *Nature* 425(6954):184-188.

AJ Bell, and TJ Sejnowski, 1995. An Information-Maximization Approach to Blind Separation and Blind Deconvolution. *Neural Computation* 7(6):1129-1159.

AL Shelton and JDE Gabrieli, 2002. Neural correlates of encoding space from route and survey perspectives. *The Journal of Neuroscience*, 22(7):2711-2717.

BM Jong et al., 1994. The cerebral activity related to the visual perception of forward motion in depth. *Brain*, 117(5):1039.

C Jutten et al., 1991. Blind separation of sources, Part 1: an adaptive algorithm based on neuromimetic architecture. *Signal Process*, 24(1):1-10.

CT Lin et al., 2005. EEG-based drowsiness estimation for safety driving using independent component analysis. *IEEE Transactions on Circuits and Systems I: Regular Papers*, 52(12):2726-2738.

DT Field et al., 2007. Neural Systems in the Visual Control of Steering. *Journal of Neuroscience*, 27(30):8002-8010.

E Mellet et al., 2000. Neural Correlates of Topographic Mental Exploration: The Impact of Route versus Survey Perspective Learning. *NeuroImage*, 12(5):588-600.

EA Maguire et al., 1998. Knowing where and getting there: a human navigation network. *Science*, 280(5365):921-924.

EA Maguire et al., 2006. Navigation around London by a taxi driver with bilateral hippocampal lesions. *Brain*, 129(11):2894-2907.

ER Kandel et al., 2000. Principles of Neural Science. 4th ed. McGraw-Hill Medical.

F Lacquaniti, 1997. Frames of reference in sensorimotor coordination. Handbook of Neuropsychology, 11:27–64.

G Buzs Àki, 2005. Theta rhythm of navigation: Link between path integration and landmark navigation, episodic and semantic memory. *Hippocampus*, 15(7):827-840.

G Committeri et al., 2004. Reference Frames for Spatial Cognition: Different Brain Areas are Involved in Viewer-, Object-, and Landmark-Centered Judgements About Object Location. *Journal of Cognitive Neuroscience*, 16(9):1517-1535.

G Galati et al., 2000. The neural basis of egocentric and allocentric coding of space in humans: a functional magnetic resonance study. *Experimental Brain Research*, 133(2):156-164.

G Gr Én et al., 2000. Brain activation during human navigation: gender-different neural networks as substrate of performance. *Nature Neuroscience*, 3(4):404-408.

G Janzen and M van Turennout, 2004. Selective neural representation of objects relevant for navigation. *Nature Neuroscience*, 7(6):673-677.

G Pfurtscheller et al., 1996. Post-movement beta synchronization. A correlate of an idling motor area?. *Electroencephalography and Clinical Neurophysiology*, 98(4):281-293.

G Pfurtscheller et al., 1996. Event-related synchronization (ERS) in the alpha band -- an electrophysiological correlate of cortical idling: A review. International Journal of *Psychophysiology*, 24(1-2):39-46.

GR Fink et al., 2003. Performing allocentric visuospatial judgments with induced distortion of the egocentric reference frame: an fMRI study with clinical implications. *NeuroImage*, 20(3):1505-1517.

G Vallar et al., 1999. A fronto-parietal system for computing the egocentric spatial frame of reference in humans. *Experimental Brain Research*, 124(3):281-286.

IP Howard and WB Templeton, 1966. Human Spatial Orientation. John Wiley and Sons Ltd.

JB Caplan et al., 2003. Human theta Oscillations Related to Sensorimotor Integration and Spatial Learning. *Journal of Neuroscience*, 23(11):4726-4736.

JR Pani and D Dupree. 1994. Spatial reference systems in the comprehension of rotational motion. *Perception*, 23(8):929-946.

JA Pineda, 2005. The functional significance of mu rhythms: Translating seeing and hearing into doing. *Brain Research Reviews*, 50(1):57-68.

K Gramann et al., 2006. The neural basis of ego- and allocentric reference frames in spatial navigation: Evidence from spatio-temporal coupled current density reconstruction. *Brain Research*, 1118(1):116-129.

K Jordan et al., 2004. Different cortical activations for subjects using allocentric or egocentric strategies in a virtual navigation task. *Neurorepor*, 15(1):135-40.

M Moscovitch et al., 2005. Functional neuroanatomy of remote episodic, semantic and spatial memory: a unified account based on multiple trace theory. *Journal of Anatomy*, 207(1):35.

M Moscovitch et al., 2006. The cognitive neuroscience of remote episodic, semantic and spatial memory. *Current Opinion in Neurobiology*, 16(2):179-190.

MC Morrone et al., 2000. A cortical area that responds specifically to optic flow, revealed by fMRI. *Nature Neuroscience*, 3:1322-1328.

M Naganawa et al., 2005. Extraction of a plasma time-activity curve from dynamic brain PET images based on independent component analysis. *IEEE Transactions on Biomedical Engineering*, 52(2):201-210.

MJ Kahana et al., 1999. Human theta oscillations exhibit task dependence during virtual maze navigation. *Nature*, 399(6738):781-784.

NR Cooper et al., 2006. Investigating evoked and induced electroencephalogram activity in task-related alpha power increases during an internally directed attention task. *NeuroReport*, 17(2):205-208.

NR Cooper et al., 2003. Paradox lost? Exploring the role of alpha oscillations during externally vs. internally directed attention and the implications for idling and inhibition hypotheses. *International Journal of Psychophysiology*, 47(1):65-74.

N Nishiyama et al. 2002. Theta episodes observed in human scalp EEG during virtual navigation-spatial distribution and task dependence. In Neural Information Processing, 2002. ICONIP '02. 428-432.

P Comon, 1994. Independent Component Analysis, A new concept?. *Signal Processing*, 36(3):287-314.

P Dourish and M Chalmers, 1994. Running Out of Space: Models of Information Navigation, short paper. HCI'94.

PE Gilbert et al., 1998. Memory for spatial location: role of the hippocampus in mediating spatial pattern separation. *Journal Neuroscience*, 18(2):804-10.

RP Darken and B Peterson, 2001. Spatial Orientation, Wayfinding, and Representation.

RL Klatzky, 1998. Allocentric and Egocentric Spatial Representations: Definitions, Distinctions, and Interconnections. *Spatial Cognition*, 1-17.

RP Darken and JL Sibert, 1996. Wayfinding strategies and behaviors in large virtual worlds. *In Proceedings of R the SIGCHI conference on Human factors in computing systems: common ground, Vancouver, British Columbia, Canada: ACM*, p. 142-149.

R Liao et al., 2005. An information-theoretic criterion for intrasubject alignment of FMRI time series: motion corrected independent component analysis. *IEEE Transactions on Medical Imaging*, 24(1):29-44.

R Salmelin and R Hari, 1994. Spatiotemporal characteristics of sensorimotor neuromagnetic rhythms related to thumb movement. *Neuroscience*, 60(2):537-50.

RS Rosenbaum et al., 2000. Remote spatial memory in an amnesic person with extensive bilateral hippocampal lesions. *Nature Neuroscience*, 3(10):1044–1048.

S Raghavachari et al., 2001. Gating of human theta oscillations by a working memory task. *Journal of Neuroscience*, 21(9):3175-3183.

S Sdoia et al., 2004. Opposite visual field asymmetries for egocentric and allocentric spatial judgments. *NeuroReport*, 15(8):1303-1305.

S Blakemore and U Frith, 2005. The learning brain. Oxford, Blackwell Publishing.

S Makeig, 1993. Auditory Event-Related Dynamics of the EEG Spectrum and Effects of Exposure to Tones. *Electroencephalography and Clinical Neurophysiology*, 86:283-293.

S Makeig et al., 1996. Independent Component Analysis of Electroencephalographic Data. *Cognitive Brain Research*, 8(1):145-151.

S Makeig and TP Jung, 1996. Tonic, phasic, and transient EEG correlates of auditory awareness in drowsiness. *Cognitive Brain Research*, 4(1):15-25.

TH Donner et al., 2007. Population Activity in the Human Dorsal Pathway Predicts the Accuracy of Visual Motion Detection. *Journal of Neurophysiology*, 98(1):345-359.

TP Jung et al., 2000, Removing Electroencephalographic Artifacts by Blind Source Separation. *Psychophysiology*, 37(02):163-178.

TW Lee et al., 1999. Independent Component Analysis Using an Extended Infomax Algorithm for Mixed Subgaussian and Supergaussian Sources. *Neural Computation*, 11(2):417-441.

T Zaehle et al., 2007. The neural basis of the egocentric and allocentric spatial frame of reference. *Brain Research*, 1137:92-103.

W Klimesch et al., 2007. EEG alpha oscillations: The inhibition-timing hypothesis. *Brain Research Reviews*, 53(1):63-88.